Molecular Biology of the Cell
Vol. 21, 1072–1087, March 15, 2010

Members of the RSC Chromatin-Remodeling Complex Are Required for Maintaining Proper Nuclear Envelope Structure and Pore Complex Localization

Laura C. Titus,* T. Renee Dawson,* Deborah J. Rexer,* Kathryn J. Ryan,† and Susan R. Wente

Department of Cell and Developmental Biology, Vanderbilt University School of Medicine, Nashville, TN 37232-8240

Submitted July 27, 2009; Revised December 8, 2009; Accepted January 15, 2010
Monitoring Editor: Yixian Zheng

The assembly, distribution, and functional integrity of nuclear pore complexes (NPCs) in the nuclear envelope (NE) are key determinants in the nuclear periphery architecture. However, the mechanisms controlling proper NPC and NE structure are not fully defined. We used two different genetic screening approaches to identify *Saccharomyces cerevisiae* mutants with defects in NPC localization. The first approach examined green fluorescent protein (GFP)-Nic96 in 531 strains from the yeast Tet-promoters Hughes Collection with individual essential genes expressed from a doxycycline-regulated promoter (*$TetO_7$-orf*). Under repressive conditions, depletion of the protein encoded by 44 *$TetO_7$-orf* strains resulted in mislocalized GFP-Nic96. These included *STH1*, *RSC4*, *RSC8*, *RSC9*, *RSC58*, *ARP7*, and *ARP9*, each encoding components of the RSC chromatin remodeling complex. Second, a temperature-sensitive *sth1-F793S* (*npa18-1*) mutant was identified in an independent genetic screen for NPC assembly (*npa*) mutants. NPC mislocalization in the *RSC* mutants required new protein synthesis and ongoing transcription, confirming that lack of global transcription did not underlie the phenotypes. Electron microscopy studies showed significantly altered NEs and nuclear morphology, with coincident cytoplasmic membrane sheet accumulation. Strikingly, increasing membrane fluidity with benzyl alcohol treatment prevented the *sth1-F793S* NE structural defects and NPC mislocalization. We speculate that NE structure is functionally linked to proper chromatin architecture.

INTRODUCTION

The nuclear envelope (NE) double lipid bilayer is a defining feature of the eukaryotic cell, imparting spatial separation between the nuclear chromatin and the cytoplasm. As such, knowing how communication across the NE is mediated will be critical to resolving regulation of gene expression and nucleocytoplasmic signaling. Nuclear pore complexes (NPCs) constitute the site of exchange for all macromolecules between the nucleus and cytoplasm. Each NPC spans a NE pore and consists of a central channel, cytoplasmic and nuclear ring structures, cytoplasmic fibrils, and a nucleoplasmic basket-like structure (Beck *et al*., 2004). The composition of the metazoan and budding yeast NPC has been analyzed by multiple groups, and overall both are built from a similar complexity of ~30 total conserved proteins, referred to as nucleoporins (Nups) and pore membrane proteins (Poms) (Rout *et al*., 2000; Cronshaw *et al*., 2002; reviewed in Tran and Wente, 2006). Some Nups are present exclusively on one face of the NPC, and others on both faces (Rout *et al*., 2000; Fahrenkrog and Aebi, 2003). Recent studies have revealed connections between nuclear face Nups and chromatin (reviewed in Capelson and Hetzer, 2009) and between NE dynamics and NPCs (Scarcelli *et al*., 2007). Understanding the structural organization and biogenesis of the NE and NPCs is required to more fully define functional events at the nuclear periphery.

In higher eukaryotes, NPCs assemble at the end of an open mitosis as the NE reforms (Hetzer *et al*., 2005). Importantly, NPCs also are generated de novo in the existing NE during interphase with the number of NPCs nearly doubling (Maul *et al*., 1971). In organisms with a closed mitosis, such as the budding yeast *Saccharomyces cerevisiae*, an intact NE is maintained throughout the entire cell cycle and all NPC biogenesis requires de novo insertion into this preexisting NE (Winey *et al*., 1997). Therefore, the NE must be plastic and dynamic for these de novo events of NPC assembly, while simultaneously functioning to preserve the structural integrity of the nucleus. Remarkably, the NE in *S. cerevisiae* lacks the structural support provided by the nuclear lamins in metazoans and still retains a spherical nuclear shape with a nonrandom distribution of NPCs (Winey *et al*., 1997).

Recent evidence suggests that several factors converge to control NE dynamics at sites of de novo NPC assembly. Such new NPCs arise by insertion and not by the duplication and division of existing NPCs (D'Angelo *et al*., 2006). First, reorganization and fusion of the NE to form a pore is probably initiated from both sides of the double membrane by

This article was published online ahead of print in *MBC in Press* (http://www.molbiolcell.org/cgi/doi/10.1091/mbc.E09–07–0615) on January 28, 2010.

* These authors contributed equally to this work.

† Present address: Department of Biology, Texas A&M University, 3258 TAMU, College Station, TX 77843-3258.

Address correspondence to: Susan R. Wente (susan.wente@vanderbilt.edu).

Abbreviations used: BA, benzyl alcohol; GFP, green fluorescence protein; GPI, glycosylphosphatidyl inositol; HU, hydroxyurea; NE, nuclear envelope; NPC, nuclear pore complex; Nup, nucleoporin; ORF, open reading frame; Pom, pore membrane protein; TBZ, thiabendazole; TEM, transmission electron microscopy.

the Poms: Pom34, Pom152, and Ndc1 in *S. cerevisiae* and Pom121, gp210, and Ndc1 in higher eukaryotes (Aitchison *et al.*, 1995; Lau *et al.*, 2004; Antonin *et al.*, 2005; Campbell *et al.*, 2006; Madrid *et al.*, 2006; Mansfeld *et al.*, 2006; Miao *et al.*, 2006; Stavru *et al.*, 2006; Dawson *et al.*, 2009; Onischenko *et al.*, 2009). Second, several Nups with predicted COPII/coatomer-like domains are implicated in stabilizing these pore membranes, including the yeast Nup84 (metazoan Nup107-160) subcomplex (Siniossoglou *et al.*, 1996; Harel *et al.*, 2003; Walther *et al.*, 2003; D'Angelo *et al.*, 2006; Devos *et al.*, 2006; Drin *et al.*, 2007; Hsia *et al.*, 2007; Brohawn *et al.*, 2008; Debler *et al.*, 2008), yeast Nup53-Nup59 (metazoan Nup32) (Marelli *et al.*, 2001; Hawryluk-Gara *et al.*, 2008; Onischenko *et al.*, 2009), and yeast Nup170-Nup157 (Flemming *et al.*, 2009; Makio *et al.*, 2009). Notably, Nup53-Nup59 and Nup170-Nup157 also have discrete connections to the Poms. Nup53-Nup59 interact physically with Ndc1 (Mansfeld *et al.*, 2006; Onischenko *et al.*, 2009) and genetically with Pom34 (Miao *et al.*, 2006); whereas Nup170-Nup157 exhibits both genetic and physical interactions with Pom34 and Pom152 (Aitchison *et al.*, 1995; Tcheperegine *et al.*, 1999; Miao *et al.*, 2006; Flemming *et al.*, 2009; Makio *et al.*, 2009). Known to maintain endoplasmic reticulum (ER) tubules (De Craene *et al.*, 2006; Voeltz *et al.*, 2006; Hu *et al.*, 2008), yeast *RTN1* and *YOP1* also have genetic linkages to both the *POM*s and genes encoding the yeast Nup84 subcomplex (Dawson *et al.*, 2009). Moreover, loss of Rtn1 and Yop1 results in dramatic alterations of NPC morphology and localization and reduced pore formation in vitro. These discoveries underscore the importance of controlling NE dynamics for NPC assembly.

Several ER/NE integral membrane proteins that affect NE composition or fluidity also impact NPC structure. NPCs are mislocalized into NE herniations in *brr6* and *apq12* mutants (de Bruyn Kops and Guthrie, 2001; Scarcelli *et al.*, 2007), and the membrane fluidizing agent benzyl alcohol rescues the *apq12* phenotype (Scarcelli *et al.*, 2007). Interestingly, flares of NE-containing NPCs develop in yeast strains lacking the Spo7/Nem1 holoenzyme, a negative regulator of phospholipid synthesis (Siniossoglou *et al.*, 1998; Campbell *et al.*, 2006). These NE/NPC flares expand directly from the NE region nearest the nucleolus, suggesting that both phospholipid composition and chromatin interactions impact NE and NPC dynamics.

For postmitotic NE and NPC assembly, recent studies have suggested that the chromatin-associated factor MEL-28/ELYS is required for Nup107-160 complex targeting (Rasala *et al.*, 2006; Franz *et al.*, 2007; Gillespie *et al.*, 2007; Liu *et al.*, 2009). The AT-rich hook of MEL-28/ELYS binds to AT-rich chromatin, and Nup107-160 binding facilitates recruitment of vesicles containing Pom121 and Ndc1 (Rasala *et al.*, 2008). This might reflect the recruitment of Nups to condensed chromatin and formation of a "prepore" structure. Moreover, such prepores could trigger nuclear pore formation coincident with postmitotic NE reformation (Anderson and Hetzer, 2008). A similar requirement for Nup–chromatin interactions in biogenesis during de novo NPC insertion into intact NEs has not been reported.

Here, we used a combination of innovative genetic approaches in *S. cerevisiae* to comprehensively assess the role of essential factors in NPC localization, structure, and potentially assembly into the NE. The genes identified encode factors involved in nuclear transport, chromatin remodeling, secretion, lipid anchoring, protein degradation, and lipid biosynthesis. Strikingly, multiple components of the RSC chromatin remodeling complex were identified including the essential ATPase catalytic subunit Sth1 (Du *et al.*, 1998). In *S. cerevisiae*, the RSC complex is composed of 15 subunits, several of which are essential for cell viability (Cairns *et al.*, 1996; Martens and Winston, 2003; Sahaa *et al.*, 2006). Although RSC was first identified for its roles in chromatin remodeling and has been linked to transcriptional activation and inhibition (Cairns *et al.*, 1996; Angus-Hill *et al.*, 2001; Damelin *et al.*, 2002; Ng *et al.*, 2002; Kasten *et al.*, 2004; Soutourina *et al.*, 2006), RSC has also been linked to a wide range of chromatin-based functions such as kinetochore function and cohesin association (Hsu *et al.*, 2003; Baetz *et al.*, 2004; Huang *et al.*, 2004) and double-strand break repair with the DNA damage response (Chai *et al.*, 2005; Shim *et al.*, 2005, 2007; Liang *et al.*, 2007). Several reports suggest connections between NPCs and RSC. A *nup84*Δ *rsc7*Δ double mutant is synthetically lethal (Wilson *et al.*, 2006), and an *rsc9* mutant has altered Kap121-GFP localization (Damelin *et al.*, 2002). In this report, we present evidence for the role of the RSC complex in maintaining proper NE and NPC structure.

MATERIALS AND METHODS

Yeast Strains, Plasmids, Genetics, and Media

All *S. cerevisiae* strains used in this study are listed in Table 1. The original *npa18-1* strain (SWY3201) was backcrossed with the parental strain SWY2090 to yield SWY3202 (temperature sensitive at 34°C and GFP-Nup mislocalization). A *LEU2/CEN* library (American Type Culture Collection, Manassas, VA) was transformed into the SWY3202 strain, and colonies were incubated at the permissive temperature, 23°C, for 36 h and then shifted to 34°C. Plasmid DNA was recovered from each resulting colony and analyzed by restriction digest. The library plasmid inserts from two independent isolates were sequenced. The minimal overlapping region harbored only two complete open reading frames (ORFs), *STH1* and *YIL127C*. Wild-type *STH1* and *YIL127C*, with respective flanking promoter regions, were independently subcloned into the XbaI and XhoI sites of pRS315 (Sikorski and Hieter, 1989) by polymerase chain reaction (PCR) amplification using library plasmid template and the following forward and reverse primers, respectively: *STH1*, 5′-CAAGTCTAGACCTGTCGATTAACTGAGC-3′ and 5′-GTAACTCGAGCTAGAAAGAGTATTAGAGG-3′ and *YIL127C*, 5′-ACGTTCTAGACGAACAACTTAAGGAGGGAG-3′ and 5′-GCAACTCGAGTTCACATTGATGAGCACGTG-3′. The resulting p*STH1* (pSW3051) and p*YIL127C* (pSW3049) plasmids were transformed into SWY3202. To analyze the *sth1* allele in SWY3202, genomic DNA from the mutant strain was amplified using *STH1* flanking oligonucleotides and the high-fidelity polymerase *Pfu* (Stratagene, La Jolla, CA). Products from two independent PCR reactions were purified and sequenced.

All strains were cultured in either rich (YPD: 1% yeast extract, 2% peptone, and 2% dextrose) or synthetic minimal (SM) media lacking appropriate amino acids and supplemented with 2% dextrose. All yeast genetic techniques and molecular cloning were performed according to standard procedures (Sherman *et al.*, 1986; Sambrook *et al.*, 1989). Cell viability assays were performed on treated and untreated *sth1-F793S* and the *TetO$_7$-STH1* mutant strains. After growth under permissive and nonpermissive conditions (3 and 12 h, respectively), the mutant strains were plated onto YP plates at 100 cells per plate, incubated at 23°C for 2 d, and quantified for colony-forming units. Serial dilutions of mid-log phase W303, SWY4143, S288C, and BLY49 were spotted onto YP plates supplemented with 2% glucose, 2% galactose, 2% raffinose or 2% ethanol/2% glycerol. These strains were also spotted onto YPD plates containing thiabendazole (TBZ; 60 μg/ml) or hydroxyurea (HU; 50 mM). The plates were imaged after 3 d incubation at the semipermissive temperatures of the respective mutant alleles. Multicopy suppressor plasmids from were obtained from the Yeast Genomic Tiling Collection through Open Biosystems (Huntsville, AL) (Jones *et al.*, 2008).

TetO$_7$-Promoter GFP-nic96 Strain Collection Generation

The yeast Tet-promoters Hughes Collection (referred to here as the *TetO$_7$-orf* strain collection) was obtained from Open Biosystems (Mnaimneh *et al.*, 2004). This collection contains 813 strains of the 1105 reported total essential genes. By a series of strain crosses and selections, *GFP-nic96* was incorporated into each *TetO$_7$-orf* strain that was reported as having a slow growth phenotype on doxycycline. Strain Y3656 was crossed with SWY2090 (Table 1). The resulting strain, SWY3191, was crossed with strains from the *TetO$_7$-orf* strain collection. Strains were mated on YPD for a minimum of 6 h, and diploids were selected by pinning three successive times onto SM Lys$^-$His$^-$ media. For sporulation, strains were incubated on YPD for 15 h at 30°C and then transferred by pinning to SPO media (1% potassium acetate, 0.1% yeast extract, 0.05% glucose, 14 mg/l histidine, and 71 mg/l leucine). Diploids were allowed to sporulate at 23°C for at least 4 d. *MATα* haploids were selected by streaking each strain to SM Arg$^-$Leu$^-$Can$^+$ (60 mg/l canavanine sulfate)

Table 1. Yeast strains used in this study

Strain	Genotype	Source
$TetO_7$ collection	*MATa CAN1 his3 leu2 met15 URA3::CMV-tTA orf::kanR-tetO$_7$-TATA*	Open Biosystems Mnaimneh *et al*. (2004)
Y3656	*MATα can1Δ::MFA1pr-HIS3::MFα1pr-LEU2 ura3Δ0 lys2Δ0 leu2Δ0 his3Δ1*	Tong *et al*. (2004)
W303	*MATa ade2-1 can1-100 his3-11,15 leu2-3,112 trp1-1 ura3-1*	Thomas *et al*. (1989)
S288C	*MATa ura3-52 his3Δ200 ade2-101 lys2-801*	Mortimer and Johnston (1986)
SWY2090	*MATa GFP-nic96:HIS3 nup170-GFP:URA3 trp1-1 ura3-1 his3-11,15 leu2-3,112 can1-100 ade2-1::ADE2:ura3*	Ryan and Wente (2002)
SWY2324	*MATα sec13-G176R (npa2-1) GFP-nic96:HIS3 nup170-GFP:URA3 lys2 ura3-1 his3-11,15 leu2-3,112 can1-100 ade2-1::ADE2:ura3*	Ryan and Wente (2002)
SWY2325	*MATα sec23-S383L (npa1-1) GFP-nic96:HIS3 nup170-GFP:URA3 lys2 ura3-1 his3-11,15 leu2-3,112 can1-100 ade2-1::ADE2:ura3*	Ryan and Wente (2002)
SWY2518	*MATa prp20-G282S (npa14-1) trp1-1 ura3-1 his3-11,15 leu2-3,112 can1-100 ade2-1::ADE2:ura3*	Ryan *et al*. (2003)
SWY3191	*MATα can1Δ::MFA1pr-HIS3::MFα1pr-LEU2 GFP-nic96:HIS3 ura3 lys2 leu2 his3 ADE2*	Y3656 × SWY2090
SWY3201	*MATα sth1-F793S (npa18-1) GFP-nic96:HIS3 nup170-GFP:URA3 lys2 ura3-1 his3-11,15 leu2-3,112 can1-100 ade2-1::ADE2:ura3*	Original *npa* screen isolate Ryan and Wente (2002)
SWY3202	*MATa sth1-F793S (npa18-1) GFP-nic96:HIS3 nup170-GFP:URA3 lys2 trp1-1 ura3-1 his3-11,15 leu2-3,112 can1-100 ade2-1::ADE2:ura3*	Backcross of SWY3201 × SWY2090
SWY3243	*MATα sth1-F793S (npa18-1) GFP-nic96:HIS3 nup170-GFP:URA3 lys2 ura3-1 his3-11,15 leu2-3,112 can1-100 ade2-1::ADE2:ura3*	Backcross of SWY3201 × SWY2090
SWY3244	*MATa sth1-F793S (npa18-1) GFP-nic96:HIS3 nup170-GFP:URA3 trp1-1 ura3-1 his3-11,15 leu2-3,112 can1-100 ade2-1::ADE2:ura3*	Backcross of SWY3201 × SWY2090
SWY3249	*MATa sth1-F793S (npa18-1) trp1-1 ura3-1 his3-11,15 leu2-3,112 can1-100 ade2-1::ADE2:ura3*	SWY3243 × SWY518
SWY3250	*MATα sth1-F793S (npa18-1) lys2 ura3-1 his3-11,15 leu2-3,112 can1-100 ade2-1::ADE2:ura3*	SWY3243 × SWY518
SWY3378	*MATa sth1-F793S (npa18-1) GFP-nic96:HIS3 nup170-GFP:URA3 trp1-1 ura3-1 his3-11,15 leu2-3,112 can1-100 ade2-1::ADE2:ura3*	SWY3243 × SWY2090
SWY3409	*MATα sth1-F793S (npa18-1) prp20-G282S (npa14-1) lys2 ura3-1 his3-11,15 leu2-3,112 can1-100 ade2-1::ADE2:ura3*	SWY3250 × SWY2518
SWY3436	*MATα sec13-G176R (npa2-1) sth1-F793S (npa18-1) lys2 ura3-1 his3-11,15 leu2-3,112 can1-100 ade2-1::ADE2:ura3 GFP-nic96:HIS3 nup170-GFP: URA3*	SWY2324 × SWY3378
SWY3437	*MATα sec23-S383L (npa1-1) sth1-F793S (npa18-1) lys2 ura3-1 his3-11,15 leu2-3,112 can1-100 ade2-1::ADE2:ura3 GFP-nic96:HIS3 nup170-GFP: URA3*	SWY2325 × SWY3378
SWY4143	*MATa sth1-F793S (npa18-1) trp1-1 ura3-1 his3-11,15 leu2-3,112 can1-100 ade2-1::ADE2:ura3*	SWY3250 backcrossed 5 times to SWY518
SWY4182	*MATa sth1-F793S (npa18-1) nup60-GFP:HIS3 trp1-1 ura3-1 his3-11,15 leu2-3,112 can1-100 ade2-1::ADE2:ura3*	*nup60-GFP:HIS3* integrated into SWY4143
SWY4183	*MATa sth1-F793S (npa18-1) nup133-GFP:HIS3 trp1-1 ura3-1 his3-11,15 leu2-3,112 can1-100 ade2-1::ADE2:ura3*	*nup133-GFP:HIS3* integrated into SWY4143
SWY4184	*MATa sth1-F793S (npa18-1) nic96-GFP:HIS3 trp1-1 ura3-1 his3-11,15 leu2-3,112 can1-100 ade2-1::ADE2:ura3*	*nic96-GFP:HIS3* integrated into SWY4143
SWY4185	*MATa sth1-F793S (npa18-1) pom34-GFP:HIS3 trp1-1 ura3-1 his3-11,15 leu2-3,112 can1-100 ade2-1::ADE2:ura3*	*pom34-GFP:HIS3* integrated into SWY4143
SWY4243	*MATa sth1-F793S (npa18-1) rpb4::KAN^R nic96-GFP:HIS3 trp1-1 ura3-1 his3-11,15 leu2-3,112 can1-100 ade2-1::ADE2:ura3*	*rpb4::KAN^R* integrated into SWY4184
SWY4245	*MATa sth1-F793S (npa18-1) rpb4::KAN^R nup133-GFP:HIS3 trp1-1 ura3-1 his3-11,15 leu2-3,112 can1-100 ade2-1::ADE2:ura3*	*rpb4::KAN^R* integrated into SWY4183
SWY4247	*MATa sth1-F793S (npa18-1) rpb4::KAN^R nup60-GFP:HIS3 trp1-1 ura3-1 his3-11,15 leu2-3,112 can1-100 ade2-1::ADE2:ura3*	*rpb4::KAN^R* integrated into SWY4182
SWY4374	*MATa nup60-GFP:HIS3 ade2-1 can1-100 his3-11,15 leu2-3,112 trp1-1 ura3-1*	*nup60-GFP:HIS3* integrated into W303
SWY4375	*MATa nic96-GFP:HIS3 ade2-1 can1-100 his3-11,15 leu2-3,112 trp1-1 ura3-1*	*nic96-GFP:HIS3* integrated into W303
BLY47	*MATα sth1-1ts ade2-1 can1-100 his3-11,15 leu2-3,112 trp1-1 ura3-1*	Du *et al*. (1998)
BLY48	*MATα sth1-2ts ura3-52 his3Δ200 lys2-801 suc2*	Du *et al*. (1998)
BLY49	*MATa sth1-3ts ura3-52 his3Δ200 ade2-101*	Du *et al*. (1998)
BLY491	*MATα sth1-L1346A ura3-52 lys-801 his3Δ200*	Huang *et al*. (2004)

media. Strains with the *TetO$_7$* promoter were selected by streaking on YPD media containing G418 (200 μg/ml active units). Strains expressing the tetracycline transactivator (tTA) and *GFP-nic96* were further identified by growth on SM Ura$^-$His$^-$Leu$^-$ media. Resulting strains had the genotype *MATα can1Δ::MFA1pr-HIS3::MF*αpr-LEU2 GFP-Nic96:HIS3 URA3::CMV-tTA gene::kan^R*-tetO7-TATA leu2 his3* (*LYS or lys; TRP or trp; ADE2 or ade2-1::ADE2:ura3*). Some *GFP-nic96 TetO$_7$-orf* strains were not obtained due to apparent technical difficulties with incorporating *GFP-nic96* into the given background.

Screening the GFP-nic96 TetO$_7$-orf Strain Collection

GFP-Nic96 localization was screened visually in 531 *GFP-nic96 TetO$_7$-orf* strains after growth in doxycycline containing media. Specifically, the strains

Table 2. Results of *TetO$_7$-orf* strain phenotypes for GFP-Nic96 mislocalization

Gene	GFP-Nic96 defect[a]	Growth defect[b]	Protein description[c]
Chromatin linked			
STH1	Moderate ML	Severe	RSC complex ATPase
RSC4	Weak ML	Weak	RSC complex
RSC8	Severe ML	Severe	RSC complex
RSC9	Weak ML	Moderate	RSC complex DNA binding protein
RSC58	Moderate ML	Severe	RSC complex
ARP7/RSC11	Weak rim clusters	Severe	RSC and SWI/SNF complexes
ARP9/RSC12	Weak ML	CSG	RSC and SWI/SNF complexes
SPT16	Weak rim clusters	Severe	Remodeling and PolII elongation
TAF6	Weak speckles	Severe	Chromatin modification
DNA2	Severe distorted rim	Severe	DNA repair
Protein degradation			
UFD1	Moderate speckles	Severe	protein degradation
CDC48	Moderate ML	Severe	ATPase involved in protein degradation
PRE6	Weak speckles	Severe	20S proteosome subunit
RPN5	Moderate ML	Severe	26S proteosome regulatory subunit
Lipid synthesis			
LCB2	Weak speckles	Severe	Sphingolipid biosynthesis
FAS2	Moderate speckles	Severe	Fatty acid synthase complex
CDS1	Weak speckles	Severe	Phospholipid biosynthesis
Secretory pathway			
COP1	Moderate speckles	Severe	COPI coat
RET3	Weak speckles	Severe	COPI coat
SAR1	Moderate speckles	Severe	COPII coat
SEC10	Moderate speckles	Severe	Exocyst complex
SEC13	Weak speckles	Severe	COPII complex; Nup84 complex
SEC14	Moderate speckles	Severe	Golgi plasma membane transport
SEC15	Moderate speckles	Severe	Exocyst complex
SEC17	Weak speckles	Severe	ER-Golgi transport, cis-SNARE complex
SEC21	Weak speckles	Severe	COPI coat, ER-Golgi transport
SEC26	Weak speckles	Severe	COPI coat, ER-Golgi transport
SEC27	Weak speckles	Severe	COPI coat, ER-Golgi/Golgi-ER transport
COG4/SEC38	Moderate speckles	Severe	Fusion of transport vesicles to Golgi
YIP1	Moderate speckles	Moderate	COPII transport vesicle biogenesis
SED5	Weak speckles	Severe	t-SNARE syntaxin, ER-Golgi transport
TIP20	Weak speckles	Severe	COPI vesicle fusion with ER
BET1	Weak speckles	Severe	v-SNARE, ER-Golgi transport
Nucleoporins			
NUP145	Severe ML	Severe	Nup84 complex
NUP1	Severe distorted rim	CSG	Nuclear face, FG Nup
NUP49	Weak ML	Moderate	Nic96/Nsp1 complex, FG Nup
Nuclear transport			
RNA1	Severe clusters	Severe	Ran GTPase activating protein
PDS1	Weak ML	Severe	Karyopherin, protein import
GPI anchoring			
CDC91/GAB1	Weak speckles	Severe	Attachment of GPI anchor to proteins
YNL158W/PGA1	Weak speckles	Severe	Mannosyltransferase complex, GPI anchoring
Other			
RIB7	Weak speckles	Severe	Riboflavin biosynthesis
YNL149C/PGA2	Moderate speckles	Severe	Mitochondrion organization/biogenesis
STT4	Weak ML	Severe	PI4 kinase, vacuole morphology
TUB4	Weak speckles	Severe	Spindle organization and biogenesis

[a] GFP fluorescence in the presence of doxycycline ranked as weak, moderate, or severe in regard to mislocalization from rim (ML, lack of strong nuclear rim), speckles (small foci away from the nuclear rim), clusters (dots on the nuclear rim), or generally distorted nuclear rims that were still evenly stained with GFP-Nic96.

[b] Growth defect in the presence of doxycycline as observed in this study or as reported in Hughes *et al*. (2000).

[c] As reported in the *S. cerevisiae* Genome Database (www.yeastgenome.org).

described as having constitutive slow growth (CSG) or having a weak, moderate, or severe growth defect in media containing 10 μg/ml doxycycline (Table 2) were inoculated directly into YPD media containing 10 μg/ml doxycycline and cultured overnight (13–15 h) at 30°C. For strains with a growth phenotype described as "very severe" or "very severe/(almost) no growth on doxycycline" (Mnaimneh *et al*., 2004), log phase cultures in YPD were treated with 10 μg/ml doxycycline for ~5 h. Some of the strains with "very severe" growth defects grew sufficiently in the presence of doxycycline overnight, and were screened under these conditions.

Fluorescence, Indirect Immunofluorescence, and Electron Microscopy

Yeast strains with GFP-tagged Nups were examined from cultures by direct fluorescence microscopy. For cycloheximide, thiolutin, and benzyl alcohol experiments, logarithmically growing cultures were treated with 10 μg/ml cycloheximide, 3 μg/ml thiolutin, or 0.4% benzyl alcohol and then temperature shifted for 5 h at 34°C or treated with 10 μg/ml doxycycline for 8 to 12 h. Cell cycle arrest experiments included a 2 d preincubation with nocodazole

(15 μg/ml) followed by a 3 h shift to 34°C. Arrest was monitored with quantification of the percentages of G2-arrested cells in treated and untreated cultures, both before and after the temperature shift. For indirect immunofluorescence microscopy, cells from logarithmically growing cultures were pelleted; fixed for 10 min at room temperature with 3.7% formaldehyde, 10% methanol in 100 mM potassium phosphate, pH 6.5; and processed as described previously (Wente *et al*., 1992). Samples were incubated with affinity-purified, rabbit anti-Nup116 C-terminal polyclonal antibody (Iovine *et al*., 1995) (1:50). Bound antibody was detected by incubation with Alexa 594 goat anti-rabbit secondary antibody (1:400). Additional samples were incubated with mouse anti-Nup159 monoclonal antibody (1:10; a gift from G. Blobel and M. Rout (Rockefeller University, New York, NY), and bound antibody was detected with Alexa 594 goat anti-mouse secondary antibody (1:200).

A final stain for 5 min with 0.1 μg/ml 4,6-diamidino-2-phenylindole (DAPI) in phosphate-buffered saline (PBS), 1% bovine serum albumin was conducted before mounting onto slides with 90% glycerol, 1 mg/ml *p*-phenylenediamine, and PBS, pH 9.0. Light microscopy was performed with a BX50 microscope (Olympus, Tokyo, Japan) with a UPlanF1 100×/1.30 oil immersion objective. Images were collected with a CoolSNAP HQ camera and MetaVue version 4.6 software (Photometrics, Tucson, AZ) and processed with Photoshop 9.0 software (Adobe Systems, Mountain view, CA). For electron microscopy, 2×10^8 logarithmically growing cells were harvested from the specific culture conditions and processed as described previously (Wente and Blobel, 1993). Samples were analyzed on a CM-12 120-keV electron microscope (FEI, Hillsboro, OR). Images were acquired with an Advantage HR or MegaPlus ES 4.0 camera (Advanced Microscopy Techniques, Danvers, MA) and processed with Photoshop 9.0 software.

Invertase Assays

Cells were prepared as described previously (Ryan and Wente, 2002), except that 20 μl of cell suspension was used for each assay. Strains assayed included SWY2089 (parental), SWY3378 [*sth1-F793S (npa18-1)*], SWY2324 [*sec13-G176R (npa2-1)*], and SWY2325 [*sec23-S383L (npa1-1)*]. The percentage of activity in each sample was calculated relative to the activity of the wild-type control strain. All assays were performed on three replicate cultures.

Immunoblotting

Cultures were grown to early log phase at 23°C and then shifted to growth at 34°C in the presence or absence of 0.4% benzyl alcohol. Total cell lysates were prepared by bead beating in lysis buffer (20 mM Tris, pH. 6.5, 5 mM $MgCl_2$, 2% Triton X-100, and 150 mM NaCl) and resolved by SDS-polyacrylamide gel electrophoresis (PAGE). The blots were incubated with either affinity purified rabbit anti-Dbp5 polyclonal antibody (1:1000; Bolger *et al*., 2008) (as a loading control) or a rabbit anti-Sth1 polyclonal antibody (1:100; Saha *et al*., 2002), followed by incubation with horseradish peroxidase-conjugated anti-rabbit antibodies (Jackson ImmnoResearch Laboratories, West Grove, PA) and detection via SuperSignal West Pico enhanced chemiluminescence substrate (Pierce Chemical, Rockford, IL).

Quantitative PCR

Cells were grown to early log phase and shifted to 34°C with the addition of thiolutin (3 μg/ml). After 3 h, cells were rinsed with ice-cold sterile water and frozen in liquid nitrogen. RNA was isolated from equivalent cell numbers with hot phenol (Geng and Tansey, 2008). Oligo(dT) reverse-transcription was performed with TaqMan reverse-transcription kit (Applied Biosystems, Foster City, CA), and quantitative PCR was performed in triplicate using iCycler and iQ SYBR Green Supermix (Bio-Rad Laboratories, Hercules, CA). The comparative C_T method was used to quantify fold changes in *NUP-GFP* transcripts relative to *ACT1*. Gene-specific primers for *GFP* and *ACT1* were validated across 6 logs of input cDNA: *ACT1*, 5′-CTCCACCACTGCTGAAAGAGAA-3′ and 5′-CGAAGTCCAAGGCGACGTAA-3′ and *GFP*, 5′-AGTGGAGAGGGTGAAGGTGA-3′ and 5′-GTTGGCCATGGAACAGGTAG-3′.

RESULTS

Genome-wide Genetic Screen for Essential Regulators of GFP-Nup Localization

To identify essential factors required for NPC localization, structure, and/or assembly, we designed a genetic screening approach in the budding yeast *S. cerevisiae*. The rationale for the screen was based on extensive genetic evidence showing that mutants with defects in NPC assembly or stability have GFP-Nup mislocalization (Bucci and Wente, 1998; Ryan and Wente, 2002; Ryan *et al*., 2003, 2007; Madrid *et al*., 2006; Miao *et al*., 2006). This can be due to the inability of the GFP-Nup to incorporate into newly forming NPCs or the disassembly of existing NPCs. We hypothesized that the genes encoding regulators of the essential NPC structure would themselves be essential for viability. A collection of yeast strains has been generated wherein 813 of the 1105 reported essential genes in *S. cerevisiae* were individually placed under the control of a doxycycline-regulated promoter, $TetO_7$ (Mnaimneh *et al*., 2004). The $TetO_7$-promoter allows regulated transcription of the respective gene (*orf*) with specific repression in the presence of doxycycline. The availability of this collection enabled the design of a direct genome-wide strategy to analyze the effective null or hypomorph phenotype of known essential genes for defects in NPC structure/assembly.

To conduct the screen, a GFP-tagged allele of the essential nucleoporin *NIC96* (*GFP-nic96*) was systematically incorporated into individual doxycycline-sensitive strains of the yeast $TetO_7$-*orf* strain collection (see *Materials and Methods*). Specifically, the screen used only the $TetO_7$-*orf* strains with a reported slow growth phenotype in the presence of doxycycline (Mnaimneh *et al*., 2004). Perturbations in growth rate indicated that the essential gene was indeed down-regulated. We speculated that if the gene played a role in NPC structure/assembly, then the GFP-Nic96 localization should be perturbed when the given $TetO_7$-*orf* strain was grown in doxycycline. The resulting *GFP-nic96* $TetO_7$-*orf* strains were individually examined for GFP-Nic96 localization based on direct fluorescence microscopy of live cells. Strains were cultured in the presence of doxycycline for 5 h or overnight. In total, GFP-Nic96 localization was evaluated in 531 strains and compared with that in a parental control strain without a $TetO_7$-*orf*. GFP-Nic96 localization was scored as wild type if the fluorescent signal was detected at the nuclear rim and as mislocalized if all or a portion of the fluorescent signal was not at the nuclear rim. Mislocalization phenotypes were further ranked as weak, moderate, or severe. In addition, some strains were scored as having speckles (small foci of fluorescent signal in the cytoplasm) or as having foci/clusters of fluorescent signal at the nuclear rim.

We identified 44 $TetO_7$-*orf* strains with mislocalized GFP-Nic96 and/or distorted nuclear rim structure (Figure 1A and Table 2). Based on functional analysis in published studies, these genes were classified into eight major categories. This included genes encoding known Nups as well as factors required for nuclear transport (Ran/Kap), chromatin remodeling, secretion, protein degradation, glycosylphosphatidyl inositol (GPI) anchoring, and lipid biosynthesis. Previous studies have also documented NPC and NE perturbations in mutants with defective Nups/Poms (Wente and Blobel, 1993; Bogerd *et al*., 1994; Doye *et al*., 1994; Wente and Blobel, 1994; Aitchison *et al*., 1995; Heath *et al*., 1995; Siniossoglou *et al*., 1996; Kosova *et al*., 1999; Madrid *et al*., 2006; Miao *et al*., 2006), secretion factors (Nanduri *et al*., 1999; Nanduri and Tartakoff, 2001; Ryan and Wente, 2002), lipid biosynthetic enzymes (Schneiter *et al*., 1996), the RanGTPase cycle (Ryan *et al*., 2003), and Kap95 (Ryan *et al*., 2007). A small subset of the components known to affect NPC structure or assembly were not identified by our screen, including the Nups *NDC1*, *NUP1*, *NUP159*, and *NUP192*, as well as the RAN cycle members *NTF2* and *RNA1*. *KAP95* and *KAP121* were unresponsive to doxycycline treatment, whereas *PRP20* and *GSP1* were absent from the collection; therefore, these candidates were not included in the screen data set.

Interestingly, the screen identified genes encoding several essential components of the RSC chromatin remodeling complex: *STH1*, *RSC8*, *RSC58*, and *ARP9*. *RSC4*, *RSC9*, and *ARP7* were also identified after direct testing. Each of these strains showed GFP-Nic96 mislocalization to varying extents (Figure 1B and Table 2), which generally correlated with the growth defect of the strain in doxycycline-containing media. The level of growth in the presence of doxycy-

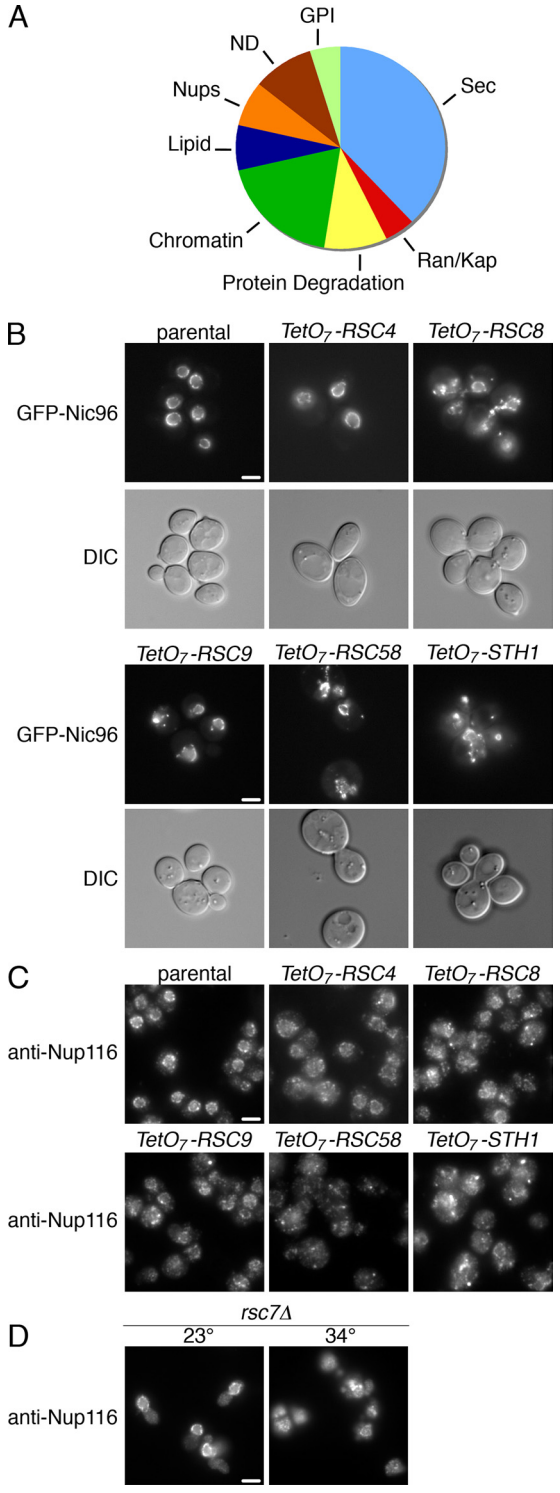

Figure 1. GFP-Nic96 mislocalizes in *TetO$_7$-orf* strains. (A) Pie chart representing the distribution between different classes of *TetO$_7$-orf* isolates with GFP-Nic96 perturbations. Genes linked to vesicular trafficking (Sec; blue), Ran/Kap (red), protein degradation (yellow), chromatin associated/chromatin remodeling (Chromatin; dark green), lipid biosynthesis (Lipid; purple), Nups (orange), others of defined function but unrelated to preceding (ND; brown), and GPI anchoring (GPI; light green). (B) Direct fluorescence microscopy of GFP-Nic96 localization in strains from the *GFP-Nic96 TetO$_7$-orf* collection is shown after growth in the presence of 10 μg/ml doxycycline for ~14 h. Differential interference contrast (DIC) images reveal cell morphology. (C and D) Indirect immunofluorescence microscopy for Nup116 localization of *TetO$_7$-orf* strains (C) after culturing in doxycycline (as in B) and the *rsc7*Δ strain (D) at 23°C and after shifting to 34°C for 5 h. Bars, 5 μm.

cline is thought to reflect the level of transcriptional repression for the respective *TetO$_7$-orf* (Mnaimneh *et al.*, 2004). Mislocalization and growth defects were severe in the *TetO$_7$-RSC58*, *TetO$_7$-RSC8*, and *TetO$_7$-STH1* strains. Mislocalization of GFP-Nups in *TetO$_7$-STH1* cells was first apparent after 6 h of culturing in the presence of doxycycline. This mislocalization became more extensive after 12 h and was detected in >90% of the cells. At this time point, viability assays confirmed that mislocalization was not an indirect effect of doxycycline toxicity or cell death (data not shown).

To further analyze the localization of NPC proteins in the *TetO$_7$-orf* strains for the RSC complex, the respective strains were processed for indirect immunofluorescence microscopy for Nup116 (Figure 1C). The *TetO$_7$-RSC8*, *TetO$_7$-RSC58*, and *TetO$_7$-STH1* strains showed severe mislocalization of Nup116 when grown in the presence of doxycycline. The *TetO$_7$-RSC4* and *TetO$_7$-RSC9* strains were again less markedly altered. Defects in NPC structure/assembly have not been documented previously in RSC complex mutants. *STH1* encodes the essential ATPase catalytic subunit of the RSC complex, whereas *RSC4*, *RSC8*, *RSC9*, and *RSC58* encode core or accessory RSC complex components (Sahaa *et al.*, 2006). Overall, this genome-wide screening strategy identified several essential RSC components that were required for normal Nup localization.

Isolation of a Temperature-sensitive sth1-F793S (npa18-1) Mutant in a Forward Genetic Screen for NPC Structure Defects

Previously, in an independent approach for identifying factors required for NPC structure/assembly, we conducted a visual screen for temperature-sensitive strains with defective GFP-Nic96 and Nup170-GFP localization (Ryan and Wente, 2002; Ryan *et al.*, 2003, 2007). This screen isolated 121 *NP*C *a*ssembly (*npa*) mutant strains in numerous complementation groups, including those with defects in secretion factors, Ran-cycle factors, and Kap95. Here, we selected one unidentified *npa* complementation group, *npa18*, to further characterize. The *npa18-1* mutant showed some GFP-Nic96/Nup170-GFP mislocalization at 23°C, and had severe mislocalization at the nonpermissive temperature (34°C) (Figure 2A). The GFP-Nic96/Nup170-GFP signal was no longer localized around the nuclear rim; instead, the fluorescent signal was detected in large, nonuniform foci throughout the cytoplasm and surrounding the nucleus. This mislocalization was first observed after 3 h at 34°C in ~40% of cells (data not shown) and was maximal by 5 h. Cell viability assays found that mislocalization was not due to cell death. Indirect immunofluorescence detection of Nup116, Nup159, and Pom152 also showed similar mislocalization (Figure 2B and Supplemental Figure S1). Thus, multiple distinct Nup subcomplexes were perturbed in the *npa18-1* mutant.

Backcrossing the *npa18-1* mutant with the parental strain revealed 2:2 linked segregation of temperature sensitivity and GFP-Nup mislocalization. This indicated that the defects were due to the mutation of a single gene. To identify the mutated gene, a yeast *CEN* genomic library was used to select for complementation of the recessive temperature-sensitive phenotype. The inserts from two unique plasmids that rescued the temperature-sensitive growth defect were isolated from yeast and sequenced. Both contained nucleo-

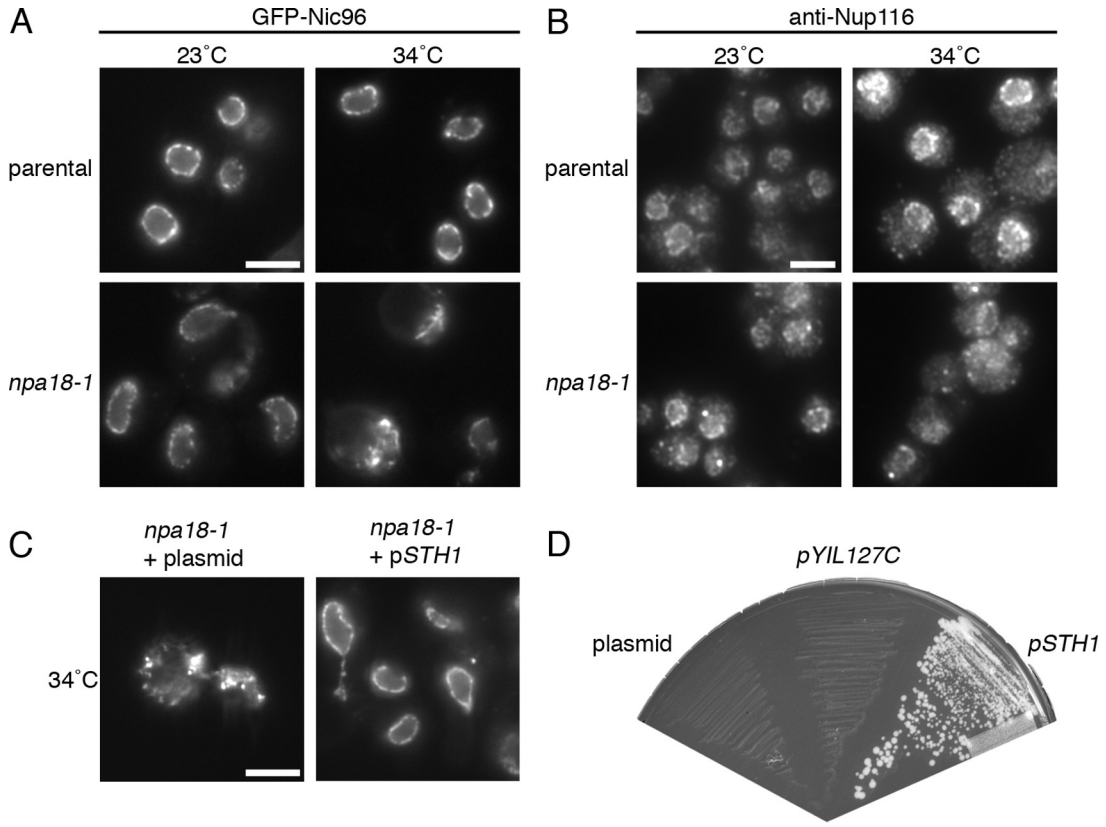

Figure 2. Nups mislocalize in the *sth1-F793S* temperature-sensitive strain. (A) Direct fluorescence microscopy of GFP-Nic96 and Nup170-GFP of logarithmically growing parental or *sth1-F793S* cells after growth at 23°C or after shifting to growth at 34°C for 5 h. Parental cells, SWY2089; *sth1-F793S GFP-nic96 nup170-GFP* cells, SWY3201. (B) Indirect immunofluorescence microscopy of *sth1-F793S* cells for Nup116 localization under the same growth conditions as described in A. Parental cells, SWY518; *sth1-F793S*, SWY3249. (C) *STH1* expression rescues the GFP-Nic96 and Nup170-GFP mislocalization in the *sth1-F793S* mutant. Direct fluorescence microscopy was conducted with the *sth1-F793S GFP-nic96 nup170-GFP* strain (SWY3202) transformed with empty plasmid (pRS315) or the *STH1* plasmid (pSW3051). Bars (A–C), 5 μm. (D) *STH1* expression rescues the *npa18-1* growth defect at 34°C. The *sth1-F793S* mutant strain (SWY3203) was transformed with empty plasmid (pRS315), plasmid harboring the *STH1* ORF and its 5′ promoter region (pSW3051), or the *YIL127C* ORF and its 5′ promoter region (pSW3049). The resulting strains were streaked for growth on SM −Leu plates.

tide sequence corresponding to a portion of chromosome IX that contained the complete ORF for *STH1* and a putative ORF *YIL127C*. Expression of *YIL127C* alone did not complement the growth defect (Figure 2D). However, an expression plasmid with *STH1* alone was necessary and sufficient for restoration of growth (Figure 2D). Furthermore, *STH1* expression also restored nuclear rim localization of GFP-Nic96 and Nup170-GFP at 34°C (Figure 2C). Sequencing the chromosomal DNA from the *npa18-1* mutant strain revealed a single point mutation in the *STH1* nucleotide sequence, which resulted in a single amino acid substitution, F793S, in the ATPase domain. Thus, we designated this *npa18-1* mutant as *sth1-F793S* and refer to it as such henceforth. Complementation analysis among the remaining unidentified *npa* mutant strains identified *sth1-F793S* as the only allele representing this *npa18* complementation group.

The sth1-F793S Mutant Is an Effective Null with Unique Allele-specific Effects

Previous studies of *STH1* have reported four temperature-sensitive *sth1* alleles (*sth1-1*, *sth1-2*, *sth1-3*, and *sth1-L1346A*) (Du *et al.*, 1998; Huang *et al.*, 2004). The *sth1-1*, *sth1-2*, and *sth1-3* alleles each have mutations in the sequence region corresponding to the ATPase domain, although distinct from the *sth1-F793S* allele. To determine whether these other *sth1* alleles perturb Nup localization, we conducted indirect immunofluorescence microscopy for Nup116 localization. After 4 h at 37°C, Nup116 remained predominantly at the nuclear rim in each of these strains (Figure 3A), whereas Nup116 mislocalized under similar conditions in the strain expressing *sth1-F793S* (Figure 2B). Similar results were obtained after 9 h at 37°C, with only slight mislocalization of Nup116 detectable in cells expressing *sth1-3* (data not shown). Therefore, the *sth1-F793S* allele had a specific effect on Nup localization.

We further characterized the *sth1-F793S* mutant by testing for whether known multicopy suppressors of *sth1-3* allele also suppressed the temperature sensitive phenotype and Nup mislocalization of the *sth1-F793S* allele. Genes encoding members of the cell wall integrity pathway (*MID2*, *RHO2*, *ROM2*. *PKC1*, and *WSC1*) have been shown previously to multicopy suppress the temperature-sensitive growth phenotype of the *sth1-3* allele (Chai *et al.*, 2002). However, the growth defect (data not shown) and Nup60-GFP mislocalization in the sth1-F793S mutant were not rescued by overexpression of any of these genes (Supplemental Figure S3). Therefore, the *sth1-F793S* allele may be affecting distinct or multiple functions of RSC that are not compensated for by the cell wall integrity pathway alone.

Next, we compared the *sth1-F793S* allele and the *sth1-3* allele for growth on different carbon sources and in the

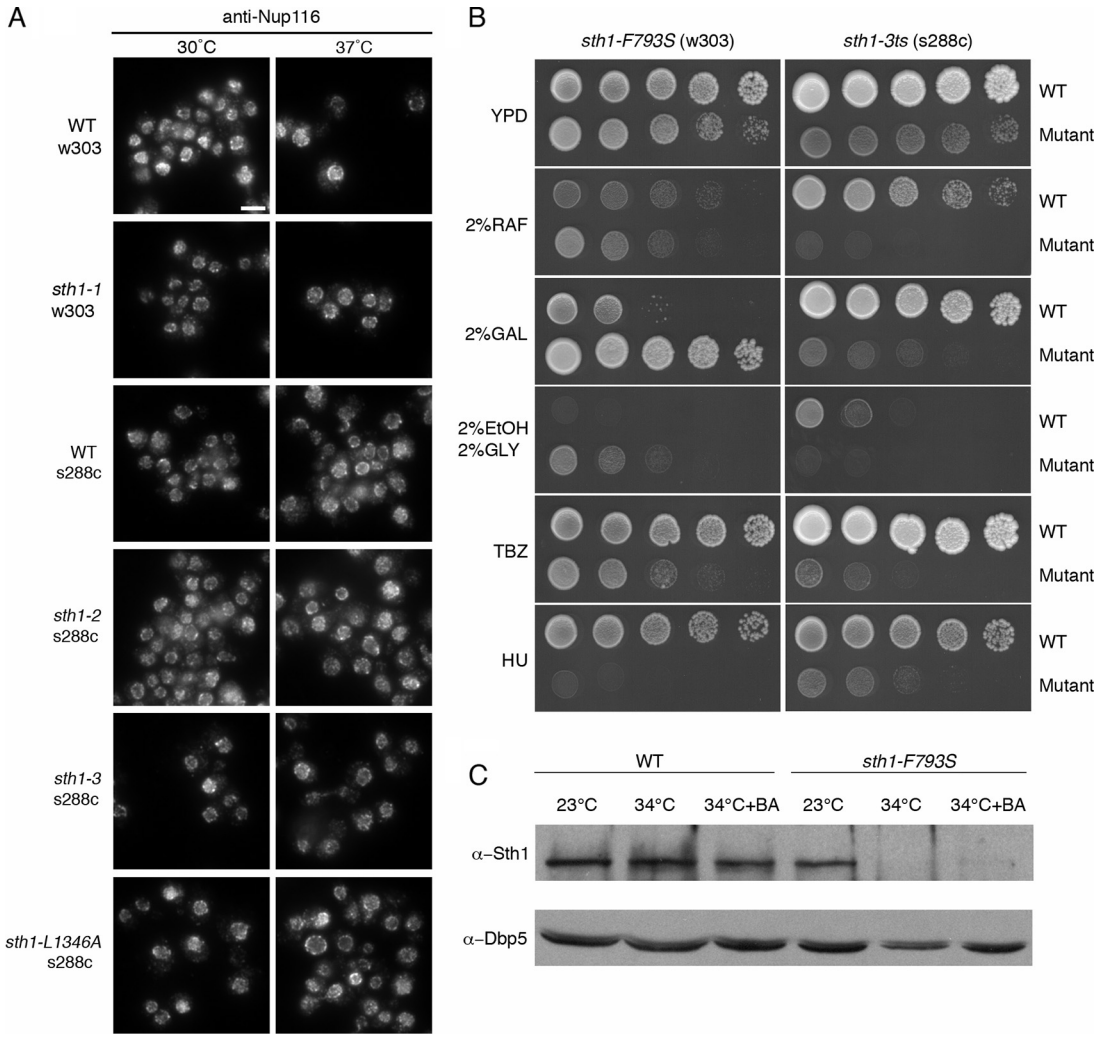

Figure 3. The *sth1-F793S* allele is distinct from other *sth1* alleles. (A) NPC mislocalization defect is specific to the *sth1-F793S* allele. Indirect immunofluorescence microscopy for Nup116 localization was conducted on logarithmically growing parental (WT) and designated *sth1* mutant cells cultured at 30°C or 37°C for 4 h. Bar, 5 μm. (B) The growth phenotypes of the *sth1-F793S* allele are distinct from those for the *sth1-3* allele. Serial diluted *sth1-F793S* and *sth1-3* mutant cells and the corresponding WT strains, W303 (SWY518), and S288C (YOL183) respectively, were spotted onto YP agar plates with different carbon sources: TBZ (60 μg/ml) or HU (50 mM). The plates were incubated at semipermissive growth temperatures (30°C for *sth1-F793S*; 35°C for *sth1-3*) and monitored for growth after 2 d. EtOH, ethanol. (C) The *sth1-F793S* allele is an effective null at 34°C. The wild-type (SWY518) and sth1-F793S (SWY4143) strains were grown for 5 h at 23 or 34°C in the presence or absence of 0.4% BA. Total cell lysates were separated by SDS-PAGE and immunoblotted with a rabbit anti-Sth1 polyclonal antibody.

presence of TBZ (microtubule-depolymerizing agent) or HU (ribonucleotide reductase inhibitor) (Figure 3B). Although the parental strains of each mutant exhibit slightly different growth phenotypes, growth of the *sth1-F793S* mutant was dramatically enhanced on nonglucose carbon sources compared with both respective parental strains and to the *sth1-3* mutant. The enhanced growth phenotype specific to the *sth1-F793S* mutant might be due to changes in transcription as a result of RSC depletion. Similar to the previously described effects on other *sth1* mutant alleles (Koyama *et al.*, 2002; Hsu *et al.*, 2003), the *sth1-F793S* mutant showed enhanced sensitivity to HU, whereas TBZ was less effective on the *sth1-F793S* mutant (Figure 3B, bottom two rows). The allele-specific drug sensitivities indicate separable functions for RSC in double-strand break repair, microtubule function and kinetochore structure (Tsuchiya *et al.*, 1998; Chai *et al.*, 2002, 2005; Shim *et al.*, 2005, 2007; Liang *et al.*, 2007).

Given the similarities between the Nup mislocalization in the *sth1-F793S* and *TetO$_7$-sth1* mutants, we evaluated protein stability in the *sth1-F793S* cells by immunoblotting. Wild-type Sth1 protein levels were unchanged after shifting to growth at 34°C for 5 h; however, the sth1-F793S protein was not detectable after temperature shifting (Figure 3C). Others report that the sth1-3 protein is stable and has wild-type ATPase activity (Du *et al.*, 1998). Thus, at 34°C, the *sth1-F793S* allele is an effective null with distinct cellular perturbations.

Analysis of Additional RSC Complex Members for NPC Perturbations

By the nature of our genetic screening strategies, all of the RSC components identified represented essential genes. To investigate other subunits, we directly examined the available null strains for nonessential RSC components (Supplemental Figure S1). Indirect immunofluorescence microscopy for anti-Nup116 and anti-GLFG Nups was conducted. Nups localized in a normal perinuclear punctate pattern in *rsc1*Δ, *rsc2*Δ, and *rsc14*Δ mutant cells. In *htl1*Δ cells, moderate mis-

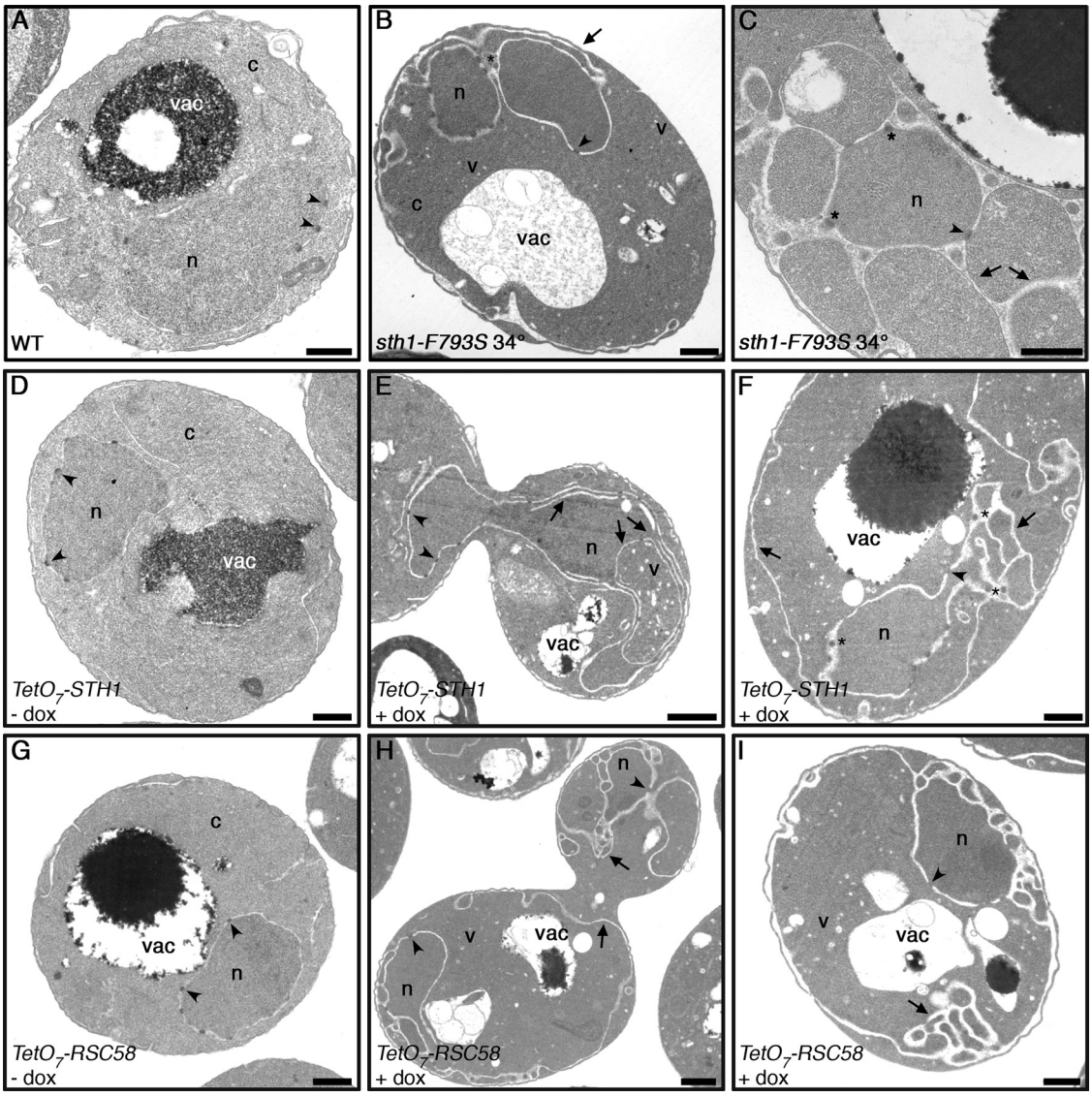

Figure 4. The *sth1-F793S* and *$TetO_7$-RSC* mutant cells have severe NE perturbations at the nonpermissive or repressive conditions. (A–C) Logarithmically growing parental cells (A; SWY2089) or *sth1-F793S* mutant cells (B and C; SWY3202) were shifted to the 34°C for 5 h and then processed for TEM. (D–I) Logarithmically growing *$TetO_7$-STH1* (D–F) and *$TetO_7$-RSC58* (G–I) cells were cultured in the absence (D and G) or presence (E, F, H, and I) of 10 μg/ml doxycycline (dox) for 10 h and then processed for thin layer TEM. n, nucleus; c, cytoplasm; vac, vacuole; v, vesicle; arrowhead, NPC; *, NPC-like structure; arrow, membrane. Bars, 0.5 μm.

localization was detected after shifting to the nonpermissive temperature. Visual scanning of the Z-plane showed severe nuclear morphology perturbations coincident with the pattern of Nup mislocalization (Supplemental Figure S1). The most striking mislocalization was observed in the *rsc7*Δ mutant, where Nups were markedly redistributed to cytoplasmic foci after shifting to growth at the nonpermissive temperature (Figure 1D). Overall, multiple independent members of the RSC complex were linked to proper NPC localization.

Ultrastructure Analysis of Nuclear Membrane Defects in sth1-F793S, $TetO_7$-STH1, and $TetO_7$-RSC58 Mutant Cells

To further investigate the NPC defects in these *$TetO_7$-RSC* and *sth1-F793S* mutants, thin section transmission electron microscopy (TEM) was conducted. The *sth1-F793S* mutant and wild-type parental strains were evaluated before and after growth for 5 h at 34°C, whereas the *$TetO_7$-STH1* and *$TetO_7$-RSC58* strains were processed after 10 h of growth in the absence and presence of doxycycline. In the wild-type parental strain and before temperature shifting (data not shown) or doxycycline treatment, the nuclei, NEs, and NPCs of all the strains were not perturbed (Figure 4). In the control cells, the NPCs appeared as electron-dense structures spanning the NE of a single distinct nucleus (Figure 4, A, D, and G). In contrast, striking ultrastructural perturbations were observed in the temperature-arrested *sth1-F793S* cells (Figure 4, B and C) and the doxycycline-treated *$TetO_7$-STH1* (Figure 4, E and F) and *$TetO_7$-RSC58* cells (Figure 4, H and I). Relative to parental or control cells, in all three mutants, there was significant cytoplasmic membrane proliferation that seemed to originate from the ER and/or NE. Extensive sheets of membrane were present, often in multiple layers, around the cell periphery/plasma membrane, and in intertwined honeycombs. There was also an accumulation of

distinct 40- to 50-nm cytoplasmic vesicles. The nucleus itself was often difficult to clearly identify. When an apparent nuclear cross section was observed, a few electron-dense structures representing NPCs were detected. The time frame after temperature or doxycycline shifting for the appearance of these ultrastructural defects was coincident with the Nup mislocalization defects described above (Figures 1 and 2).

GFP-Nup Mislocalization in RSC Mutants Requires New Protein Synthesis and Transcription

As a test for defects in new NPC assembly versus perturbations in the stability of existing NPCs, we have previously assayed the effect of cycloheximide treatment on Nup mislocalization in *npa* mutants (Ryan *et al*., 2003, 2007). Mutants that perturb preexisting factors or NPC components will not require translation for the phenotype and will show mislocalization in the presence of cycloheximide. In contrast, mislocalization due to perturbations in de novo NPC or NE biogenesis will require translation of assembly or structural factors for accumulation of perturbed GFP-Nups, and thus will not show GFP-Nup mislocalization in cycloheximide. This is true for the NPC assembly defects documented in the *prp20-G282S (npa14-1)*, *ntf2-H104Y (npa11-1)*, *rna1-S116F (npa13-1)*, *gsp1-P162L (npa15-1)*, *kap95-E126K (npa16-1)*, and *apq12*Δ mutants (Ryan *et al*., 2003, 2007; Scarcelli *et al*., 2007). In *sth1-F793S (npa18-1)* and *rsc7*Δ mutant cells treated with cycloheximide, the GFP-Nups remained associated in a predominantly nuclear rim localization after incubation at the nonpermissive temperature (Figure 5A). Marked mislocalization was not detected. Similarly, treatment of *TetO$_7$-RSC8* cells with cycloheximide during nonpermissive growth conditions also prevented Nup mislocalization (Figure 5B). These data indicate that the defects in the *sth1-F793S*, *rsc7*Δ, and *TetO$_7$-RSC8* mutant strains required ongoing translation.

Because the RSC complex is functionally linked to gene expression (Angus-Hill *et al*., 2001; Damelin *et al*., 2002; Ng *et al*., 2002; Kasten *et al*., 2004; Soutourina *et al*., 2006; Badis *et al*., 2008; Parnell *et al*., 2008; Hartley and Madhani, 2009; Mas *et al*., 2009), we speculated that some of the defects in the *sth1-F793S* mutant might be linked to altered expression of RSC-controlled genes that encode proteins involved in NE and/or NPC biogenesis. To globally assess the role of transcription in the *sth1-F793S* Nup mislocalization phenotype, we used a RNA polymerase II temperature-sensitive mutant. The *RBP4* gene encodes a nonessential RNA polymerase II subunit (Woychik and Young, 1989); however, the *rbp4*Δ is temperature sensitive for growth above 32°C and after 45 min at 37°C, 96% of RNA polymerase II transcription is lost (Woychik and Young, 1989; Miyao *et al*., 2001). The *sth1-F793S rbp4*Δ double mutant was evaluated for NPC localization by monitoring GFP-tagged Nic96, Nup60, or Nup133 (Figure 6). After shifting to growth at 34°C for 5 h, the respective GFP-tagged Nups remained localized at the nuclear rim, and mislocalization was not detected. GFP-tagged Nups also remained rim localized in the *rpb4*Δ single mutant (data not shown). This observation was further confirmed using thiolutin, an inhibitor of global RNA synthesis. Treatment with thiolutin blocked GFP-tagged Nic96 mislocalization in *TetO$_7$-STH1* cells grown in the presence of doxycycline (Supplemental Figure S4) and GFP-tagged Nic96, Nup60, Nup133 mislocalization in the *sth1-F793S* mutant (data not shown). Together, both ongoing transcription and translation were required for the NPC/NE defects.

Control experiments were also conducted to assay for effects on mRNA stability in the *sth1-F793S* Nup mislocalization phenotype. Quantitative PCR was used to evaluate *NUP* and *ACT1* relative mRNA levels between wild-type and *sth1-F793S* mutant cells. At the permissive growth temperature, *NUP60-GFP* and *NIC96-GFP* mRNA levels did not vary $>$ 1.5-fold between wild-type and *sth1-F793S* cells. After a 3-h shift to 34°C in the presence of thiolutin, the *NUP* mRNAs examined were actually stabilized relative to *ACT1* in the *sth1-F793S* cells (*NUP60-GFP* up to 5-fold and *NIC96-*

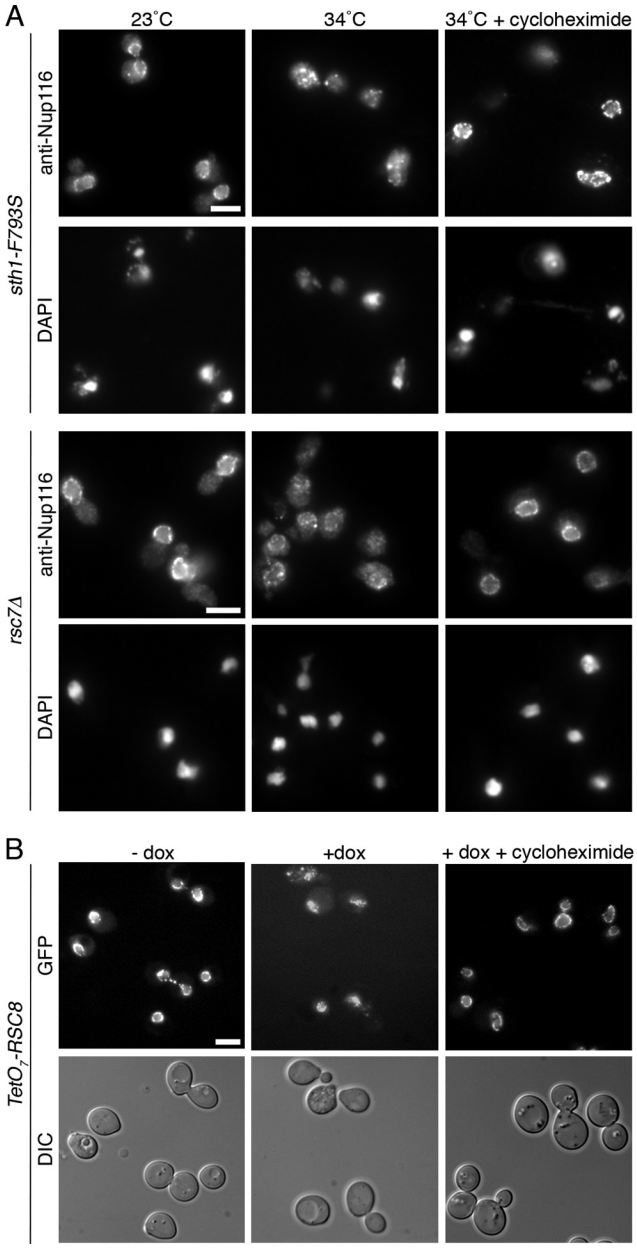

Figure 5. Translation is required for RSC NE/NPC perturbations. (A) Indirect immunofluorescence microscopy for anti-Nup116 C-terminal antibody localization was conducted for *sth1-F793S* and *rsc7*Δ mutant cells. Logarithmically growing cells were cultured at 23 or 34°C for 5 h, in the presence or absence of 10 μg/ml cycloheximide. (B) Direct fluorescence microscopy was conducted for GFP-Nic96 and Nup170-GFP localization in logarithmically growing cells *TetO$_7$-RSC8* cells cultured in the presence or absence of 10 μg/ml doxycycline (dox) and 10 μg/ml cycloheximide for 8 h. Corresponding DIC images are shown below each panel. Bars, 5 μm.

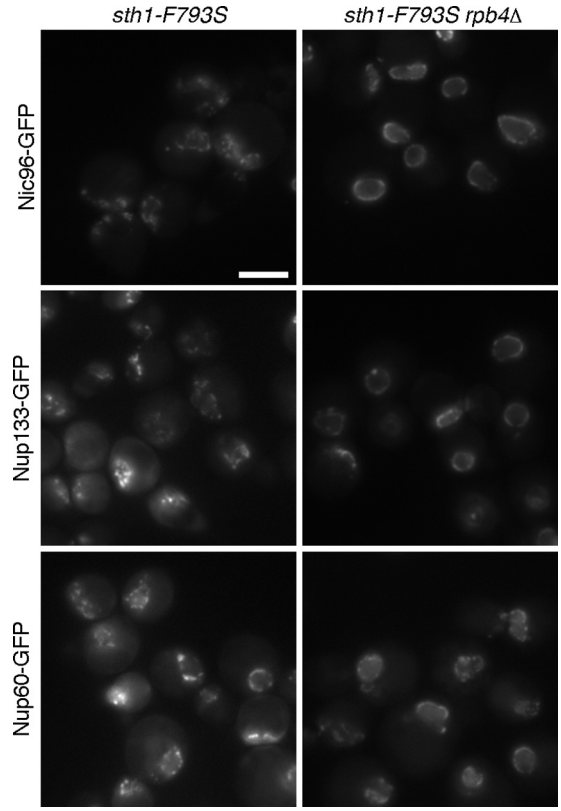

Figure 6. Nup mislocalization in *sth1-F793S* cells requires ongoing transcription. The *RPB4* deletion allele was integrated into the *sth1-F793S* strains expressing GFP-tagged Nic96 (SWY4243), Nup133 (SWY4245), or Nup60 (SWY4247). These strains and the corresponding parental *sth1-F793S RPB4* strains (SWY4244, SWY4246, and SWY4248, respectively) were shifted to 34°C for 5 h. Representative live-cell, direct fluorescence images of GFP-Nup localization are shown. Bar, 5 μm.

GFP up to 21-fold). Therefore, the lack of Nup mislocalization upon transcriptional shutoff was not due to decreased mRNA stability of the *NUP* transcripts tested.

GFP-Nup Mislocalization in the sth1-F793S Mutant Does Not Require Cell Division

To evaluate whether the transcriptional and translational shut-off were acting indirectly to block Nup mislocalization by inhibiting *sth1-F793S* cell division, we tested for mislocalization in nocodazole-arrested cells. The *sth1-F793S* mutant was treated with 15 μg/ml nocodazole for 2 h, resulting in >90% of the cells as large budded and held in G2-M. At this time point, the cultures were shifted to 34°C for 3 h. The cell population remained at >65% large-budded/G2-M. Importantly, Nup60-GFP was mislocalized to the same level in both arrested and unarrested control cultures (Supplemental Figure S5). This suggested that Nup mislocalization in *sth1-F793S* cells does not require cell division and confirmed that the lack of mislocalization in the cycloheximide, *rpb4*Δ and thiolutin experiments is linked to inhibition of translation or transcription.

Increasing Membrane Fluidity Blocks NPC/NE Defects in the sth1-F793S Mutant

Nup mislocalization and NE/ER defects have been reported in mutants defective in the RanGTPase cycle (Ryan *et al.*, 2003), in the COPII complex for ER/Golgi trafficking (Ryan and Wente, 2002), in NPC proteins (Doye and Hurt, 1995), in lipid biogenesis factors (Siniossoglou, 2009), and NE/ER membrane proteins (Scarcelli *et al.*, 2007; Dawson *et al.*, 2009). We also identified additional components in some of these pathways in the *TetO$_7$-orf* screen reported here (Figure 1A and Table 2). To directly test for links to secretion in *sth1-F793S* cells, we assayed for secreted invertase activity. The *sth1-F793S* cells displayed 53% of wild-type invertase activity relative to our parental control strain. In comparison, *sec23-S383L (npa1-1)* and *sec13-G176R (npa2-1)* mutants had 3 and 30% of wild-type invertase activity levels, respectively. We also tested for genetic interactions between the *sth1-F793S* mutant and the *sec13-G176R* or *sec23-S383L* mutant alleles. Of note, a *sth1-F793S sec13-G176R* double mutant and the *sth1-F793S sec23-S383L* double mutant were both viable and showed no synthetic fitness defects (SWY3436 and SWY3437, Table 1). The same results were found for a *sth1-F793S prp20-G282S* double mutant that was viable and showed growth identical to the *sth1-F793S* mutant (SWY3409, Table 1). We concluded that the defects in the *sth1-F793S* mutant were not due to indirect severe perturbations on the levels of secretory or RanGTPase cycle factors.

We used an independent assay to investigate whether NE membrane composition or fluidity was connected to the *sth1-F793S* mechanism of perturbation. Benzyl alcohol (BA) is an established membrane fluidizer (Colley and Metcalfe, 1972; Gordon *et al.*, 1980) that has recently been used in *S. cerevisiae* to examine the role of Apq12 in NPC assembly (Scarcelli *et al.*, 2007) and in *Aspergillus nidulans* to analyze functional roles for the An-Nup84-120 complex at the NE (Liu *et al.*, 2009). To test this with the *sth1-F793S* mutant, 0.4% BA was added to the cells coincident with the shift to the nonpermissive growth temperature. Nuclear rim localization of GFP-tagged Nic96, Nup170, Nup60, Nup133, and Pom34 were independently evaluated in respective strains by direct fluorescence microscopy (Figure 7). Strikingly, no Nup mislocalization was observed in the BA treated *sth1-F793S* cells. GFP-Nic96 was also not mislocalized when *TetO$_7$-STH1* cells were treated with BA during growth in the presence of doxycycline (Supplemental Figure S4). Moreover, TEM examination of the BA-treated, temperature-shifted *sth1-F793S* cells revealed that the ultrastructural NE defects were also absent (Figure 8). Immunoblotting was conducted and showed that the sth1-F793S protein was still unstable in the BA-treated cells (Figure 3C). Thus, the RSC role in mediating proper NE morphology and NPC localization was compensated for by alteration in NE dynamics.

DISCUSSION

In our independent *TetO$_7$-orf* and *npa* genetic screens, we find that perturbation of Sth1 and several other RSC components results in altered Nup localization, perturbed NE organization and significant cytoplasmic membrane proliferation. The comparable phenotypes between the *sth1-F793S (npa18-1)*, the *TetO$_7$-STH1*, the *TetO$_7$-RSC*, and the *rsc7*Δ mutant strains indicate that the Nup/NE perturbations result from RSC complex loss-of-function. This conclusion is further corroborated by the loss of detectable sth1-F793S protein at the nonpermissive temperature in the mutant strain. Such defects in NE/NPC structure have not been previously documented in RSC mutants. Others have found that the *rsc7(npl6)* mutant allele leads to defective localization of nuclear proteins and also have reported a genetic interaction between *rsc7* and *nup84* mutants (Bossie and Silver, 1992; Damelin *et al.*, 2002; Wilson *et al.*, 2006). We

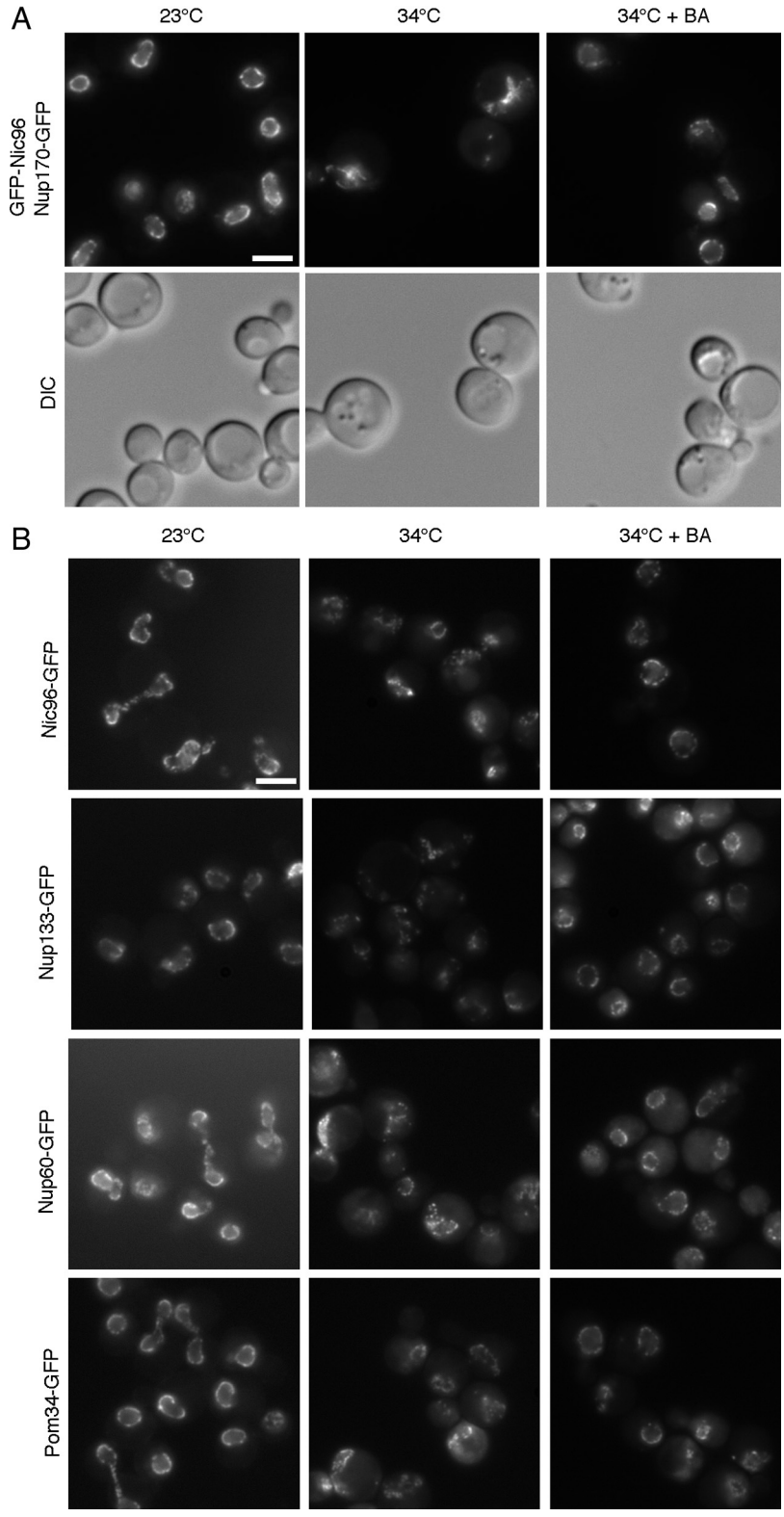

Figure 7. Benzyl alcohol treatment prevents GFP-Nup mislocalization in *sth1-F793S* cells. Logarithmically growing cultures of the *sth1-F793S GFP-nic96 nup170-GFP* (SWY3202) strain (A) and the *sth1-F793S* (SWY4143) strains with GFP-tagged Nic96, Nup60, Nup133, or Pom34 (B) were grown for 5 h at 23°C (left column) and then shifted to 34°C in the absence (middle column) or presence (right column) of 0.4% BA. Representative live-cell, direct fluorescence images of GFP-Nup localization are shown. For A, the corresponding DIC images are shown. Bars, 5 μm.

speculate that the RSC complex mutant phenotypes reflect a functional connection between proper chromatin remodeling and NE/NPC structure.

On a more general level, we have demonstrated the utility of the *TetO$_7$-orf* collection for GFP-based screening of perturbations in specific cell functions. Our prior *npa* mutant screen was not to saturation, and it would be technically challenging to achieve full genomic coverage based on the number of genes we have found with indirect perturbations in NE/NPC structure (e.g., the secretory pathway; Ryan and Wente, 2002). Taking the *TetO$_7$-orf* and *npa* screens together, we have now repeatedly identified genes in the same func-

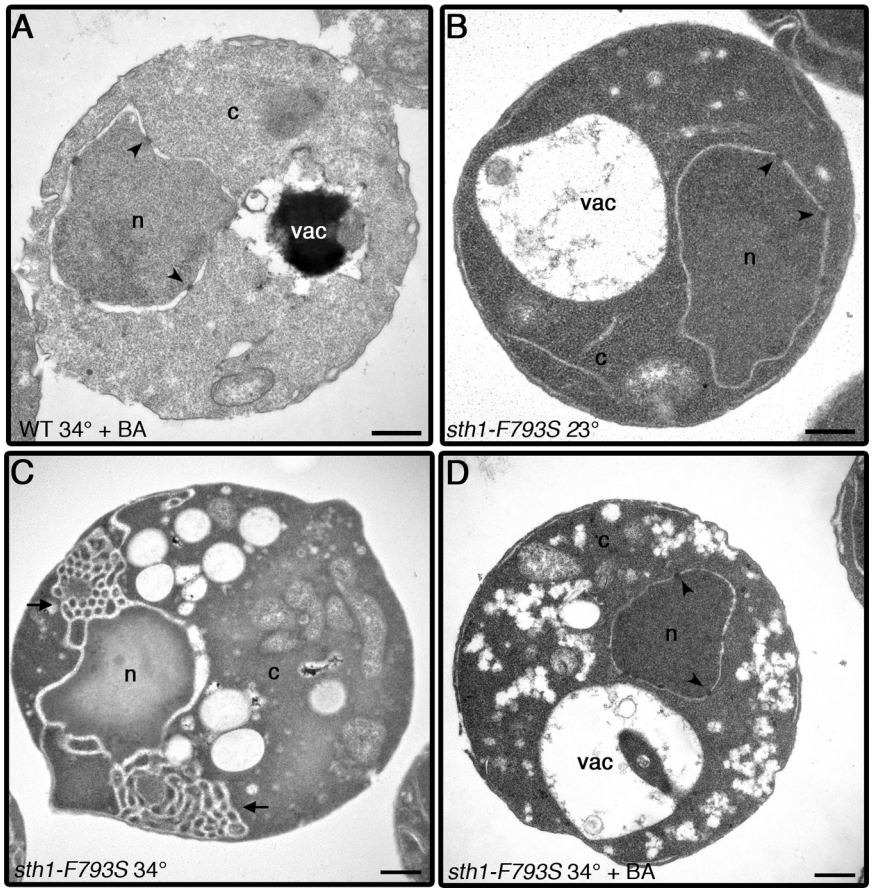

Figure 8. The *sth1-F793S* NE and nuclear morphology perturbations are prevented by benzyl alcohol. Logarithmically growing wild type (WT, SWY518) (A) and *sth1-F793S* (SWY4143) (B–D) strains were incubated for 5 h at 23°C (B) or at 34°C (A, C, and D) in the absence (C) or presence (A and D) of 0.4% BA. Samples were processed for TEM. n, nucleus; c, cytoplasm; vac, vacuole; arrowhead, NPC; arrow, membrane. Bars, 0.5 μm.

tional classes, indicating a nearly comprehensive assessment of the role of essential factors. In this study, we have further identified components of the lipid biosynthesis and secretory pathways for proper Nup localization. Others have shown that mutation of *FAS3/ACC1*, a gene required for long-chain fatty acid synthesis, results in NE/NPC defects (Schneiter *et al*., 1996). The same lipid–membrane effects might be the basis for the *TetO$_7$-LCB2*, *TetO$_7$-FAS2*, and *TetO$_7$-CDS1* defects in GFP-Nic96 localization. We also identified connections here to the proteasome and enzymes required for GPI anchoring. Future analysis of the NE and NPC defects in these mutants could give insight into the mechanisms by which the global nuclear architecture is coordinated and regulated.

Our results with the RSC complex mutants also potentially impact on prior interpretations of RSC-associated functions. Multiple studies have shown that RSC functions in DNA double-strand break repair (Chai *et al*., 2005; Shim *et al*., 2005, 2007; Liang *et al*., 2007). Interestingly, the functional integrity of two different Nup subcomplexes is required for double-strand break repair by homologous recombination (Palancade *et al*., 2007) and at least the Nup84 subcomplex is also required for anchoring telomeres and efficient DNA double-strand break repair (Therizols *et al*., 2006). Studies also report that *nup170* mutants have defects in chromosome segregation (Kerscher *et al*., 2001; Iouk *et al*., 2002). Such striking NE and NPC perturbations, and severely perturbed nuclear morphology, in the *sth1-F793S* and *TetO$_7$-RSC* cells could have indirect effects on DNA damage responses and gene expression. Additional work will be required to reveal whether some of the RSC-associated phenotypes are due to altered NE/NPCs.

We propose that there are at least two possible mechanistic explanations for the NE/NPC defects in the RSC complex mutants. First, the lack of RSC activity could result in decreased expression of a factor(s) directly required for proper NE/NPC structure and/or biogenesis, or in decreased expression of a factor(s) that maintains membrane fluidity. Others have reported that defects in the RSC complex result in pleiotropic effects attributed to either misregulated transcription or lack of chromatin access for other proteins (reviewed in Sahaa *et al*., 2006). RSC controls the transcriptional activation and repression of a broad subset of genes, with different RSC mutants having different transcriptional defects (Angus-Hill *et al*., 2001; Damelin *et al*., 2002; Ng *et al*., 2002; Kasten *et al*., 2004; Soutourina *et al*., 2006; Badis *et al*., 2008; Parnell *et al*., 2008; Hartley and Madhani, 2009). We observed that both new protein synthesis and ongoing transcription were required for the GFP-Nup perturbation, suggesting that the defects were not caused by loss of gene expression. Furthermore, we find similar NE/NPC defects in several different RSC mutants, and the *TetO$_7$-orf* screen also identified the *TetO$_7$-SPT16* and *TetO$_7$-TAF6* strains as having weak Nup localization defects. An independent study has examined strains with deleted nonessential genes and identified nuclear morphology defects in *arp5*Δ and *bre1*Δ mutants (affecting components of histone remodeling and modifying complexes) and the *seh1*Δ mutant (affecting the NPC) (Teixeira *et al*., 2002). A common silencing defect was identified among the deletion strains with altered nuclear morphology, pointing toward an interdependence between maintenance of silenced chromatin and NE structure. This indicates that the NE/NPC perturbation could be a function of the global chromatin state as opposed to a spe-

cific transcriptional defect. Our biochemical and genetic analysis of potential transcriptional targets with NPC/NE connections also suggested that the *sth1-F793S* mutant is not linked to severe indirect defects in secretion or the RanGTPase cycle. Furthermore, to date our tests of known multicopy suppressors of *sth1* mutants have not found any that rescue the altered nuclear morphology or temperature sensitivity of the *sth1-F793S* mutant. Therefore, although we cannot rule out specific changes in gene expression, we speculate that the NE/NPC defects are not simply indirect perturbations due to altered transcription levels.

As an alternative model, the RSC complex activity might be required for generating the correct chromatin state for contacts with the NE and/or association with a NE/NPC assembly factor. It has recently been shown that post-mitotic NPC assembly requires the chromatin-interacting factor MEL-28/ELYS for recruitment of the metazoan Nup107-160 complex (Rasala *et al*., 2006, 2008; Franz *et al*., 2007). In yeast, the RSC complex has been connected to the yeast Nup84 complex by its shared link to nonhomologous end-joining (NHEJ) with Nup133 and Nup120 (as well as Nup60) (Palancade *et al*., 2007). In addition, the reported synthetic lethality of a *nup84*Δ *rsc7*Δ double mutant (Wilson *et al*., 2006) further suggests that proper function of the Nup84 complex is dependent on the integrity of RSC. In this light, the connection of the RSC chromatin-remodeling complex to proper NE structure is especially intriguing. We speculate that the loss of RSC function could decouple the chromatin/NE interface, leading to a chromatin or NE stress response. Structural and/or chromatin-associated roles of Nups and Poms might be inhibited, whereas lipid biosynthetic pathways might signal to the NE to expand to reestablish chromatin connections. Indeed, several reports have shown that the nucleosome occupancy of RSC changes in response to stress (Damelin *et al*., 2002; Ng *et al*., 2002; Mas *et al*., 2009). This hypothesis is supported by our observation that increasing membrane fluidity prevented the NE and NPC perturbations in the *sth1-F793S* cells, even though the sth1-F793S protein was still absent.

Recent studies have documented connections between NPCs/Nups and transcriptional regulation (Ishii *et al*., 2002; Casolari *et al*., 2004; Rodriguez-Navarro *et al*., 2004; Dilworth *et al*., 2005; Schmid *et al*., 2006; Brown and Silver, 2007). For example, genome-wide analysis of protein:DNA binding interactions has shown that Nups preferentially bind to transcriptionally active genes and induction of *GAL* genes results in their translocation to the nuclear rim (Casolari *et al*., 2004). Two NPC nuclear basket Nups (Nup2 and Nup60) have been linked to this transcriptional regulation by their association with chromatin-bound Prp20, the RanGEF (Dilworth *et al*., 2005). Interestingly, the membrane perturbations in the *sth1-F793S* and *TetO$_7$-RSC* mutants are similar to that reported previously for *nup1* mutant cells (Bogerd *et al*., 1994), which are defective for a NPC nuclear basket Nup (Rout *et al*., 2000). There are also reported genetic interactions among components of the Nup84 complex and the Rap1 transcriptional activation complex, and most components of the Nup84 complex have the capacity to activate transcription (Menon *et al*., 2005). These data suggest that RSC might activate transcription of genes at the NPC through interactions with the Nup84 complex. Together, we conclude that a general mechanism may exist whereby the RSC complex generates a correct chromatin state for NE/NPC association, whether for transcriptional activation and/or for NE/NPC structure and biogenesis.

ACKNOWLEDGMENTS

We are indebted to G. Winfrey and G. Olson (Vanderbilt University, Nashville, TN) and to E. Woodruff (Magnify, Inc., Nashville, TN) for assistance and expertise with the electron microscopy experiments. We thank B. Laurent (Mount Sinai, New York, NY) for yeast strains, B. Cairns (University of Utah Health Sciences, Salt Lake City, Utah) for the Sth1 antibody, G. Blobel and M. Rout (The Rockefeller University, New York, NY) for the Nup159 antibody, and P. A. Weil, W. P. Tansey, and members of the Wente laboratory for critical discussion. This work was supported by National Institutes of Health grant R01 GM-57438 (S.R.W.), F32 GM-072272 (to D.J.R.), and T32 CA-09582-21 (to L.C.T.).

REFERENCES

Aitchison, J. D., Rout, M. P., Marelli, M., Blobel, G., and Wozniak, R. W. (1995). Two novel related yeast nucleoporins Nup170p and Nup157p: complementation with the vertebrate homologue Nup155p and functional interactions with the yeast nuclear pore-membrane protein Pom152p. J. Cell Biol. *131*, 1133–1148.

Anderson, D. J., and Hetzer, M. W. (2008). Reshaping of the endoplasmic reticulum limits the rate for nuclear envelope formation. J. Cell Biol. *182*, 911–924.

Angus-Hill, M. L., Schlichter, A., Roberts, D., Erdjument-Bromage, H., Tempst, P., and Cairns, B. R. (2001). A Rsc3/Rsc30 zinc cluster dimer reveals novel roles for the chromatin remodeler RSC in gene expression and cell cycle control. Mol. Cell *7*, 741–751.

Antonin, W., Franz, C., Haselmann, U., Antony, C., and Mattaj, I. W. (2005). The integral membrane nucleoporin pom121 functionally links nuclear pore complex assembly and nuclear envelope formation. Mol. Cell *17*, 83–92.

Badis, G., *et al*. (2008). A library of yeast transcription factor motifs reveals a widespread function for Rsc3 in targeting nucleosome exclusion at promoters. Mol. Cell *32*, 878–887.

Baetz, K. K., Krogan, N. J., Emili, A., Greenblatt, J., and Hieter, P. (2004). The ctf13-30/CTF12 genomic haploinsufficiency modifier screen identifies the yeast chromatin remodeling complex RSC, which is required for the establishment of sister chromatid cohesion. Mol. Cell. Biol. *24*, 1232–1244.

Beck, M., Forster, F., Ecke, M., Plitzko, J. M., Melchior, F., Gerisch, G., Baumeister, W., and Medalia, O. (2004). Nuclear pore complex structure and dynamics revealed by cryoelectron tomography. Science *306*, 1387–1390.

Bogerd, A. M., Hoffman, J. A., Amberg, D. C., Fink, G. R., and Davis, L. I. (1994). nup1 mutants exhibit pleiotropic defects in nuclear pore complex function. J. Cell Biol. *127*, 319–332.

Bolger, T. A., Folkmann, A. W., Tran, E. J., and Wente, S. R. (2008). The mRNA export factor Gle1 and inositol hexakisphosphate regulate distinct stages of translation. Cell *134*, 624–633.

Bossie, M. A., and Silver, P. A. (1992). Movement of macromolecules between the cytoplasm and the nucleus in yeast. Curr. Opin. Genet. Dev. *2*, 768–774.

Brohawn, S. G., Leksa, N. C., Spear, E. D., Rajashankar, K. R., and Schwartz, T. U. (2008). Structural evidence for common ancestry of the nuclear pore complex and vesicle coats. Science *322*, 1369–1373.

Brown, C. R., and Silver, P. A. (2007). Transcriptional regulation at the nuclear pore complex. Curr. Opin. Genet. Dev. *17*, 100–106.

Bucci, M., and Wente, S. R. (1998). A novel fluorescence-based genetic strategy identifies mutants of *Saccharomyces cerevisiae* defective for nuclear pore complex assembly. Mol. Biol. Cell *9*, 2439–2461.

Cairns, B. R., Lorch, Y., Li, Y., Zhang, M., Lacomis, L., Erdjument-Bromage, H., Tempst, P., Du, J., Laurent, B., and Kornberg, R. D. (1996). RSC, an essential, abundant chromatin-remodeling complex. Cell *87*, 1249–1260.

Campbell, J. L., Lorenz, A., Witkin, K. L., Hays, T., Loidl, J., and Cohen-Fix, O. (2006). Yeast nuclear envelope subdomains with distinct abilities to resist membrane expansion. Mol. Biol. Cell *17*, 1768–1778.

Capelson, M., and Hetzer, M. W. (2009). The role of nuclear pores in gene regulation, development and disease. EMBO Rep. *10*, 697–705.

Casolari, J. M., Brown, C. R., Komili, S., West, J., Hieronymus, J., and Silver, P. A. (2004). Genome-wide localization of the nuclear transport machinery couples transcriptional status and nuclear organization. Cell *117*, 427–439.

Chai, B., Hsu, J., Du, J., and Laurent, B. (2002). Yeast RSC function is required for organization of the cellular cytoskeleton via an alternative PKC1 pathway. Genetics *161*, 575–584.

Chai, B., Huang, J., Cairns, B. R., and Laurent, B. C. (2005). Distinct roles for the RSC and Swi/Snf ATP-dependent chromatin remodelers in DNA double-strand break repair. Genes Dev. *19*, 1656–1661.

Colley, C. M., and Metcalfe, J. C. (1972). The localisation of small molecules in lipid bilayers. FEBS Lett. *24*, 241–246.

Cronshaw, J. M., Krutchinsky, A. N., Zhang, W., Chait, B. T., and Matunis, M. J. (2002). Proteomic analysis of the mammalian nuclear pore complex. J. Cell Biol. *158*, 915–927.

D'Angelo, M. A., Anderson, D. J., Richard, E., and Hetzer, M. W. (2006). Nuclear pores form de novo from both sides of the nuclear envelope. Science *312*, 440–443.

Damelin, M., Simon, I., Moy, T. I., Wilson, B., Komilli, S., Tempst, P., Roth, F. P., Young, R. A., Cairns, B. R., and Silver, P. A. (2002). The genome-wide localization of Rsc9, a component of the RSC chromatin-remodeling complex, changes in response to stress. Mol. Cell *9*, 563–573.

Dawson, T. R., Lazarus, M. D., Hetzer, M. W., and Wente, S. R. (2009). ER membrane-bending proteins are necessary for de novo nuclear pore formation. J. Cell Biol. *184*, 659–675.

de Bruyn Kops, A., and Guthrie, C. (2001). An essential nuclear envelope integral membrane protein, Brr6p, required for nuclear transport. EMBO J. *20*, 4183–4193.

De Craene, J. O., Coleman, J., Estrada de Martin, P., Pypaert, M., Anderson, S., Yates, J. R., 3rd, Ferro-Novick, S., and Novick, P. (2006). Rtn1p is involved in structuring the cortical endoplasmic reticulum. Mol. Biol. Cell *17*, 3009–3020.

Debler, E. W., Ma, Y., Seo, H. S., Hsia, K. C., Noriega, T. R., Blobel, G., and Hoelz, A. (2008). A fence-like coat for the nuclear pore membrane. Mol. Cell *32*, 815–826.

Devos, D., Dokudovskaya, S., Williams, R., Alber, F., Eswar, N., Chait, B. T., Rout, M. P., and Sali, A. (2006). Simple fold composition and modular architecture of the nuclear pore complex. Proc. Natl. Acad. Sci. USA *103*, 2172–2177.

Dilworth, D. J., Tackett, A. J., Rogers, R. S., Yi, E. C., Christmas, R. H., Smith, J. J., Siegel, A. F., Chait, B. T., Wozniak, R. W., and Aitchison, J. D. (2005). The mobile nucleoporin Nup2p and chromatin-bound Prp20p function in endogenous NPC-mediated transcriptional control. J. Cell Biol. *171*, 955–965.

Doye, V., and Hurt, E. C. (1995). Genetic approaches to nuclear pore structure and function. Trends Genet. *11*, 235–241.

Doye, V., Wepf, R., and Hurt, E. C. (1994). A novel nuclear pore protein Nup133p with distinct roles in poly(A)+ RNA transport and nuclear pore distribution. EMBO J. *13*, 6062–6075.

Drin, G., Casella, J. F., Gautier, R., Boehmer, T., Schwartz, T. U., and Antonny, B. (2007). A general amphipathic alpha-helical motif for sensing membrane curvature. Nat. Struct. Mol. Biol. *14*, 138–146.

Du, J., Nasir, I., Benton, B. K., Kladde, M. P., and Laurent, B. C. (1998). Sth1p, a *Saccharomyces cerevisiae* Snf2p/Swi2p homolog, is an essential ATPase in RSC and differs from Snf/SWI in its interactions with histones and chromatin-associated proteins. Genetics *150*, 987–1005.

Fahrenkrog, B., and Aebi, U. (2003). The nuclear pore complex: nucleocytoplasmic transport and beyond. Nat. Rev. Mol. Cell Biol. *4*, 757–766.

Flemming, D., Sarges, P., Stelter, P., Hellwig, A., Bottcher, B., and Hurt, E. (2009). Two structurally distinct domains of the nucleoporin Nup170 cooperate to tether a subset of nucleoporins to nuclear pores. J. Cell Biol. *185*, 387–395.

Franz, C., Walczak, R., Yavuz, S., Santarella, R., Gentzel, M., Askjaer, P., Galy, V., Hetzer, M., Mattaj, I. W., and Antonin, W. (2007). MEL-28/ELYS is required for the recruitment of nucleoporins to chromatin and postmitotic nuclear pore complex assembly. EMBO Rep. *8*, 165–172.

Geng, F., and Tansey, W. P. (2008). Polyubiquitination of Histone H2B. Mol. Biol. Cell *19*, 3616–3624.

Gillespie, P. J., Khoudoli, G. A., Stewart, G., Swedlow, J. R., and Blow, J. J. (2007). ELYS/MEL-28 chromatin association coordinates nuclear pore complex assembly and replication licensing. Curr. Biol. *17*, 1657–1662.

Gordon, L. M., Dipple, I., Sauerheber, R. D., Esgate, J. A., and Houslay, M. D. (1980). The selective effects of charged local anaesthetics on the glucagon- and fluoride-stimulated adenylate cyclase activity of rat-liver plasma membranes. J. Supramol. Struct. *14*, 21–32.

Harel, A., Orjalo, A. V., Vincent, T., Lachish-Zalait, A., Vasu, S. K., Shah, S., Zimmerman, E., Elbaum, M., and Forbes, D. J. (2003). Removal of a single pore subcomplex results in vertebrate nuclei devoid of nuclear pores. Mol. Cell *11*, 853–864.

Hartley, P. D., and Madhani, H. D. (2009). Mechanisms that specify promoter nucleosome location and identity. Cell *137*, 445–458.

Hawryluk-Gara, L. A., Platani, M., Santarella, R., Wozniak, R. W., and Mattaj, I. W. (2008). Nup53 is required for nuclear envelope and nuclear pore complex assembly. Mol. Biol. Cell *19*, 1753–1762.

Heath, C. V., Copeland, C. S., Amberg, D. C., Del Priore, V., Snyder, M., and Cole, C. N. (1995). Nuclear pore complex clustering and nuclear accumulation of poly(A)+ RNA associated with mutation of the *Saccharomyces cerevisiae RAT2/NUP120* gene. J. Cell Biol. *131*, 1677–1697.

Hetzer, M., Walther, T. C., and Mattaj, I. W. (2005). Pushing the envelope: structure, function, and dynamics of the nuclear periphery. Annu. Rev. Cell Dev. Biol. *21*, 347–380.

Hsia, K. C., Stavropoulos, P., Blobel, G., and Hoelz, A. (2007). Architecture of a coat for the nuclear pore membrane. Cell *131*, 1313–1326.

Hsu, J. M., Huang, J., Meluh, P. B., and Laurent, B. C. (2003). The yeast RSC chromatin-remodeling complex is required for kinetochore function in chromosome segregation. Mol. Cell. Biol. *23*, 3202–3215.

Hu, J., Shibata, Y., Voss, C., Shemesh, T., Li, Z., Coughlin, M., Kozlov, M. M., Rapoport, T. A., and Prinz, W. A. (2008). Membrane proteins of the endoplasmic reticulum induce high-curvature tubules. Science *319*, 1247–1250.

Huang, J., Hsu, J. M., and Laurent, B. C. (2004). The RSC nucleosome-remodeling complex is required for cohesin's association with chromosome arms. Mol. Cell *13*, 739–750.

Iouk, T., Kerscher, O., Scott, R. J., Basrai, M. A., and Wozniak, R. W. (2002). The yeast nuclear pore complex functionally interacts with components of the spindle assembly checkpoint. J. Cell Biol. *159*, 807–819.

Iovine, M. K., Watkins, J. L., and Wente, S. R. (1995). The GLFG repetitive region of the nucleoporin Nup116p interacts with Kap95p, an essential yeast nuclear import factor. J. Cell Biol. *131*, 1699–1713.

Ishii, K., Arib, G., Lin, C., Van Houwe, G., and Laemmli, U. K. (2002). Chromatin boundaries in budding yeast: the nuclear pore connection. Cell *109*, 551–562.

Jones, M. G., Stalker, J., Humphray, S., West, A., Cox, T., Rogers, J., Dunham, I., and Prelich, G. (2008). A systematic library for comprehensive overexpression screens in *Saccharomyces cerevisiae*. Nat. Methods *5*, 239–241.

Kasten, M., Szerlong, H., Erdjument-Bromage, H., Tempst, P., Werner, M., and Cairns, B. R. (2004). Tandem bromodomains in the chromatin remodeler RSC recognize acetylated histone H3 Lys14. EMBO J. *23*, 1348–1359.

Kerscher, O., Hieter, P., Winey, M., and Basrai, M. A. (2001). Novel role for a *Saccharomyces cerevisiae* nucleoporin, Nup170p, in chromosome segregation. Genetics *157*, 1543–1553.

Kosova, B., Pante, N., Rollenhagen, C., and Hurt, E. (1999). Nup192p is a conserved nucleoporin with a preferential location at the inner site of the nuclear membrane. J. Biol. Chem. *274*, 22646–22651.

Koyama, H., Itoh, M., Miyahara, K., and Tsuchiya, E. (2002). Abundance of the RSC nucleosome-remodeling complex is important for the cells to tolerate DNA damage in *Saccharomyces cerevisiae*. FEBS Lett. *531*, 215–221.

Lau, C. K., Giddings, T. H., and Winey, M. (2004). A novel allele of *Saccharomyces cerevisiae NDC1* reveals a potential role for the spindle pole component Ndc1p in nuclear pore assembly. Eukaryot. Cell *3*, 447–458.

Liang, B., Qiu, J., Ratnakumar, K., and Laurent, B. C. (2007). RSC functions as an early double-strand-break sensor in the cell's response to DNA damage. Curr. Biol. *17*, 1–6.

Liu, H. L., De Souza, C. P., Osmani, A. H., and Osmani, S. A. (2009). The three fungal transmembrane nuclear pore complex proteins of *Aspergillus nidulans* are dispensable in the presence of an intact An-Nup84-120 complex. Mol. Biol. Cell *20*, 616–630.

Madrid, A. S., Mancuso, J., Cande, W. Z., and Weis, K. (2006). The role of the integral membrane nucleoporins Ndc1p and Pom152p in nuclear pore complex assembly and function. J. Cell Biol. *173*, 361–371.

Makio, T., Stanton, L. H., Lin, C. C., Goldfarb, D. S., Weis, K., and Wozniak, R. W. (2009). The nucleoporins Nup170p and Nup157p are essential for nuclear pore complex assembly. J. Cell Biol. *185*, 459–473.

Mansfeld, J., *et al*. (2006). The conserved transmembrane nucleoporin NDC1 is required for nuclear pore complex assembly in vertebrate cells. Mol. Cell *22*, 93–103.

Marelli, M., Lusk, C. P., Chan, H., Aitchison, J. D., and Wozniak, R. W. (2001). A link between the synthesis of nucleoporins and the biogenesis of the nuclear envelope. J. Cell Biol. *153*, 709–724.

Martens, J. A., and Winston, F. (2003). Recent advances in understanding chromatin remodeling by Swi/Snf complexes. Curr. Opin. Genet. Dev. *13*, 136–142.

Mas, G., de Nadal, E., Dechant, R., Rodriguez de la Concepcion, M. L., Logie, C., Jimeno-Gonzalez, S., Chavez, S., Ammerer, G., and Posas, F. (2009). Recruitment of a chromatin remodelling complex by the Hog1 MAP kinase to stress genes. EMBO J. *28*, 326–336.

Maul, G. G., Price, J. W., and Lieberman, M. W. (1971). Formation and distribution of nuclear pore complexes in interphase. J. Cell Biol. *51*, 405–418.

Menon, B. B., Sarma, N. J., Pasula, S., Deminoff, S. J., Willis, K. A., Barbara, K. E., Andrews, B., and Santangelo, G. M. (2005). Reverse recruitment: the

Nup84 nuclear pore subcomplex mediates Rap1/Gcr1/Gcr2 transcriptional activation. Proc. Natl. Acad. Sci. USA *102*, 5749–5754.

Miao, M., Ryan, K. J., and Wente, S. R. (2006). The integral membrane protein Pom34p functionally links nucleoporin subcomplexes. Genetics *172*, 1441–1457.

Miyao, T., Barnett, J. D., and Woychik, N. A. (2001). Deletion of the RNA polymerase subunit RPB4 acts as a global, not stress-specific, shut-off switch for RNA polymerase II transcription at high temperatures. J. Biol. Chem. *276*, 46408–46413.

Mnaimneh, S., *et al*. (2004). Exploration of essential gene functions via titratable promoter alleles. Cell *118*, 31–44.

Nanduri, J., MItra, S., Andrei, C., Liu, Y., Yu, Y., Hitomi, M., and Tartakoff, A. M. (1999). An unexpected link between the secretory path and the organization of the nucleus. J. Biol. Chem. *274*, 33785–33789.

Nanduri, J., and Tartakoff, A. M. (2001). The arrest of secretion response in yeast: signaling from the secretory path to the nucleus via Wsc proteins and Pkc1p. Mol. Cell *8*, 281–289.

Ng, H. H., Robert, F., Young, R. A., and Struhl, K. (2002). Genome-wide location and regulated recruitment of the RSC nucleosome-remodeling complex. Genes Dev. *16*, 806–819.

Onischenko, E., Stanton, L. H., Madrid, A. S., Kieselbach, T., and Weis, K. (2009). Role of the Ndc1 interaction network in yeast nuclear pore complex assembly and maintenance. J. Cell Biol. *185*, 475–491.

Palancade, B., Liu, X., Garcia-Rubio, M., Aguilera, A., Zhao, X., and Doye, V. (2007). Nucleoporins prevent DNA damage accumulation by modulating Ulp1-dependent sumoylation process. Mol. Biol. Cell *18*, 2912–2923.

Parnell, T. J., Huff, J. T., and Cairns, B. R. (2008). RSC regulates nucleosome positioning at Pol II genes and density at Pol III genes. EMBO J. *27*, 100–110.

Rasala, B. A., Orjalo, A. V., Shen, Z., Briggs, S., and Forbes, D. J. (2006). ELYS is a dual nucleoporin/kinetochore protein required for nuclear pore assembly and proper cell division. Proc. Natl. Acad. Sci. USA *47*, 17801–17806.

Rasala, B. A., Ramos, C., Harel, A., and Forbes, D. J. (2008). Capture of AT-rich chromatin by ELYS recruits POM121 and NDC1 to initiate nuclear pore assembly. Mol. Biol. Cell *19*, 3982–3996.

Rodriguez-Navarro, S., Fischer, T., Luo, M. J., Antunez, O., Brettschneider, S., Lechner, J., Perez-Ortin, J. E., Reed, R., and Hurt, E. (2004). Sus1, a functional component of the SAGA histone acetylase complex and the nuclear pore-associated mRNA export machinery. Cell *116*, 75–86.

Rout, M. P., Aitchison, J. D., Suprapto, A., Hjertaas, K., Zhao, Y., and Chait, B. T. (2000). The yeast nuclear pore complex: composition, architecture, and transport mechanism. J. Cell Biol. *148*, 635–651.

Ryan, K. J., McCaffery, J. M., and Wente, S. R. (2003). The Ran GTPase cycle is required for yeast nuclear pore complex assembly. J. Cell Biol. *160*, 1041–1053.

Ryan, K. J., and Wente, S. R. (2002). Isolation and characterization of new *Saccharomyces cerevisiae* mutants perturbed in nuclear pore complex assembly. BMC Genet. *3*, 17

Ryan, K. J., Zhou, Y., and Wente, S. R. (2007). The karyopherin Kap95 regulates nuclear pore complex assembly into intact nuclear envelopes in vivo. Mol. Biol. Cell *18*, 886–898.

Saha, A., Wittmeyer, J., and Cairns, B. R. (2002). Chromatin remodeling by RSC involves ATP-dependent DNA translocation. Genes Dev. *16*, 2120–2134.

Sahaa, A., Wittmeyer, J., and Cairns, B. R. (2006). Chromatin remodelling: the industrial revolution of DNA around histones. Nat. Rev. Mol. Cell Biol. *7*, 437–447.

Sambrook, J., Fritsch, E. F., and Maniatis, T. (1989). Molecular Cloning: A Laboratory Manual, Cold Spring Harbor, NY: Cold Spring Harbor Laboratory Press.

Scarcelli, J. J., Hodge, C. A., and Cole, C. N. (2007). The yeast integral membrane protein Apq12 potentially links membrane dynamics to assembly of nuclear pore complexes. J. Cell Biol. *178*, 799–812.

Schmid, M., Arib, G., Laemmli, C., Nishikawa, J., Durussel, T., and Laemmli, U. K. (2006). Nup-PI: the nucleopore-promoter interaction of genes in yeast. Mol. Cell *21*, 379–391.

Schneiter, R., Hitomi, M., Ivessa, A., Fasch, E.-V., Kohlwein, S. D., and Tartakoff, A. M. (1996). A yeast acetyl coenzyme A carboxylase mutant links very-long-chain fatty acid synthesis to the structure and function of the nuclear membrane-pore complex. Mol. Cell. Biol. *16*, 7161–7172.

Sherman, F., Fink, G. R., and Hicks, J. B. (1986). Methods in Yeast Genetics, Cold Spring Harbor, NY: Cold Spring Harbor Laboratory Press.

Shim, E. Y., Hong, S. J., Oum, J.-H., Yanez, Y., Zhang, Y., and Lee, S. E. (2007). RSC mobilizes nucleosomes to improve accessibility of repair machinery to the damaged chromatin. Mol. Cell. Biol. *27*, 1602–1613.

Shim, E. Y., Ma, J.-L., Oum, J.-H., Yanez, Y., and Lee, S. E. (2005). The yeast chromatin remodeler RSC complex facilitates end joining repair of DNA double-strand breaks. Mol. Cell. Biol. *25*, 3934–3944.

Sikorski, R. S., and Hieter, P. (1989). A system of shuttle vectors and yeast host strains designed for efficient manipulation of DNA in *Saccharomyces cerevisiae*. Genetics *122*, 19–27.

Siniossoglou, S. (2009). Lipins, lipids and nuclear envelope structure. Traffic *10*, 1181–1187.

Siniossoglou, S., Lutzmann, M., Santos-Rosa, H., Leonard, K., Mueller, S., Aebi, U., and Hurt, E. (1996). A novel complex of nucleoporins, which includes Sec13p and a Sec13p homolog, is essential for normal nuclear pores. Cell *84*, 265–275.

Siniossoglou, S., Santos-Rosa, H., Rappsilber, J., Mann, M., and Hurt, E. (1998). A novel complex of membrane proteins required for formation of a spherical nucleus. EMBO J. *17*, 6449–6464.

Soutourina, J., *et al*. (2006). Rsc4 connects the chromatin remodeler RSC to RNA polymerases. Mol. Cell. Biol. *26*, 4920–4933.

Stavru, F., Hulsmann, B. B., Spang, A., Hartmann, E., Cordes, V. C., and Gorlich, D. (2006). NDC *1*, a crucial membrane-integral nucleoporin of metazoan nuclear pore complexes. J. Cell Biol. *173*, 509–519.

Tcheperegine, S. E., Marelli, M., and Wozniak, R. W. (1999). Topology and functional domains of the yeast pore membrane protein Pom152p. J. Biol. Chem. *274*, 5252–5258.

Teixeira, M. T., Dujon, B., and Fabre, E. (2002). Genome-wide nuclear morphology screen identifies novel genes involved in nuclear architecture and gene-silencing in *Saccharomyces cerevisiae*. J. Mol. Biol. *321*, 551–561.

Therizols, P., Fairhead, C., Cabal, G. G., Genovesio, A., Olivo-Marin, J.-C., Dujon, B., and Fabre, E. (2006). Telomere tethering at the nuclear periphery is essential for efficient DNA double strand break repair in subtelomeric region. J. Cell Biol. *172*, 189–199.

Tran, E. J., and Wente, S. R. (2006). Dynamic nuclear pore complexes: life on the edge. Cell *125*, 1041–1053.

Tsuchiya, E., Hosotani, T., and Miyakawa, T. (1998). A mutation in NPS1/STH1, an essential gene encoding a component of a novel chromatin-remodeling complex RSC, alters the chromatin structure of *Saccharomyces cerevisiae* centromeres. Nucleic Acids Res. *26*, 3286–3292.

Voeltz, G. K., Prinz, W. A., Shibata, Y., Rist, J. M., and Rapoport, T. A. (2006). A class of membrane proteins shaping the tubular endoplasmic reticulum. Cell *124*, 573–586.

Walther, T. C., *et al*. (2003). The conserved Nup107-160 complex is critical for nuclear pore complex assembly. Cell *113*, 195–206.

Wente, S. R., and Blobel, G. (1993). A temperature-sensitive *nup116* null mutant forms a nuclear envelope seal over the yeast nuclear pore complex thereby blocking nucleocytoplasmic traffic. J. Cell Biol. *123*, 275–284.

Wente, S. R., and Blobel, G. (1994). NUP145 encodes a novel yeast glycine-leucine-phenylalanine-glycine (GLFG) nucleoporin required for nuclear envelope structure. J. Cell Biol. *125*, 955–969.

Wente, S. R., Rout, M. P., and Blobel, G. (1992). A new family of yeast nuclear pore complex proteins. J. Cell Biol. *119*, 705–723.

Wilson, B., Erdjument-Bromage, H., Tempst, P., and Cairns, B. R. (2006). The RSC chromatin remodeling complex bears an essential fungal-specific protein module with broad functional roles. Genetics *172*, 795–809.

Winey, M., Yarar, D., Giddings, T. H., Jr., and Mastronarde, D. N. (1997). Nuclear pore complex number and distribution throughout the *Saccharomyces cerevisiae* cell cycle by three-dimensional reconstruction from electron micrographs of nuclear envelopes. Mol. Biol. Cell *8*, 2119–2132.

Woychik, N. A., and Young, R. A. (1989). RNA polymerase II subunit RPB4 is essential for high- and low-temperature yeast cell growth. Mol. Cell. Biol. *9*, 2854–2859.